DRA

NATIONAL AERONAUTICS AND SPACE ADMINISTRATION

Technical Report 32-1600

Results of the 1973 NASA/JPL Balloon Flight Solar Cell Calibration Program

Robert K. Yasui

Richard F. Greenwood

JET PROPULSION LABORATORY

CALIFORNIA INSTITUTE OF TECHNOLOGY

PASADENA, CALIFORNIA

November 1, 1975

TECHNICAL REPORT STANDARD TITLE PAGE

1. Report No. 32-1600	2. Government Accession No.	3. Recipient's Catalog No.
4. Title and Subtitle RESULTS OF THE 1973 NASA/JPL BALLOON FLIGHT SOLAR CELL CALIBRATION PROGRAM		5. Report Date November 1, 1975 6. Performing Organization Code
7. Author(s) Robert K. Yasui, Richard F. Greenwood		8. Performing Organization Report No.
9. Performing Organization Name and Address JET PROPULSION LABORATORY California Institute of Technology 4800 Oak Grove Drive Pasadena, California 91103		10. Work Unit No. 11. Contract or Grant No. NAS 7-100 13. Type of Report and Period Covered Technical Report
12. Sponsoring Agency Name and Address NATIONAL AERONAUTICS AND SPACE ADMINISTRATION Washington, D.C. 20546		14. Sponsoring Agency Code

15. Supplementary Notes

16. Abstract

High-altitude balloon flights for solar cell calibration were resumed in November, 1973, after a three-year interval. Four flights were successfully completed, and all objectives of the flight program were met. The balloon flights were conducted by NASA/JPL through the cooperation and assistance of the National Science Foundation's National Scientific Balloon Facility located in Palestine, Texas. Each balloon flight carried 37 standard solar cells for calibration above 99.5% of the earth's atmosphere. The solar cells were assembled into standard modules with appropriate resistors to load each cell at short-circuit current. In turn, each standardized module was mounted at the apex of the balloon on a sun tracker which automatically maintained normal incidence to the sun within ±1.0 deg. The balloons were launched to reach a float altitude of approximately 36.6 km (120,000 ft) two hours before solar noon and remain at float altitude for two hours beyond solar noon. Telemetered calibration data on each standard solar cell was collected during the float period and recorded on magnetic tape.

The magnetic tape was subsequently returned to JPL for data reduction and analysis. At the end of each float period the solar cell payload was separated from the balloon by radio command and descended via parachute

17. Key Words (Selected by Author(s))	18. Distribution Statement
Spacecraft Propulsion and Power Energy Production and Conversion Solar Physics	Unclassified -- Unlimited

19. Security Classif. (of this report)	20. Security Classif. (of this page)	21. No. of Pages	22. Price
Unclassified	Unclassified	28	

TECHNICAL REPORT STANDARD TITLE PAGE

1. Report No. 32-1600	2. Government Accession No.	3. Recipient's Catalog No.
4. Title and Subtitle		5. Report Date
		6. Performing Organization Code
7. Author(s)		8. Performing Organization Report No.
9. Performing Organization Name and Address JET PROPULSION LABORATORY California Institute of Technology 4800 Oak Grove Drive Pasadena, California 91103		10. Work Unit No. 11. Contract or Grant No. NAS 7-100 13. Type of Report and Period Covered
12. Sponsoring Agency Name and Address NATIONAL AERONAUTICS AND SPACE ADMINISTRATION Washington, D.C. 20546		14. Sponsoring Agency Code
15. Supplementary Notes		

16. Abstract

to a ground recovery crew. Standard solar cells calibrated and recovered in this manner are used as primary intensity reference standards in solar simulators and in terrestrial sunlight for evaluating the performance of other solar cells and solar arrays with similar spectral response characteristics. This is now the most widely accepted technique for developing space standard solar cells in the United States.

17. Key Words (Selected by Author(s))	18. Distribution Statement		
19. Security Classif. (of this report)	20. Security Classif. (of this page)	21. No. of Pages	22. Price

NATIONAL AERONAUTICS AND SPACE ADMINISTRATION

Technical Report 32-1600

Results of the 1973 NASA/JPL Balloon Flight Solar Cell Calibration Program

Robert K. Yasui
Richard F. Greenwood

JET PROPULSION LABORATORY
CALIFORNIA INSTITUTE OF TECHNOLOGY
PASADENA, CALIFORNIA

November 1, 1975

Preface

The work described in this report was performed by the Guidance and Control Division of the Jet Propulsion Laboratory. The report describes the modified balloon flight system and the results of three out of four planned series of balloon flights conducted with the cooperation of the National Center for Atmospheric Research (NCAR), National Scientific Balloon Facility (NSBF), located in Palestine, Texas.

Acknowledgment

The authors wish to express their appreciation for the services, cooperation, and support provided by the National Center for Atmospheric Research, National Scientific Balloon Facility staff. A. Shipley, R. Kubara, B. Cunningham, E. Smith, and L. Vice were among those who were especially helpful.

The authors also wish to thank the following JPL people: R. L. Mueller, R. S. Weiss, and J. K. Person, for their careful fabrication of solar cell modules, accurate solar cell measurements, and maintenance of the associated electronic equipment; L. Fite, who assisted greatly with the development of the computer program; and E. N. Costogue, who performed the system error analysis. The cooperation and patience extended by all the organizations who participated were much appreciated.

Contents

Tables

Figures

Abstract

High-altitude balloon flights for solar cell calibration were resumed in November, 1973, after a three-year interval. Four flights were successfully completed, and all objectives of the flight program were met. The balloon flights were conducted by NASA/JPL through the cooperation and assistance of the National Science Foundation's National Scientific Balloon Facility located in Palestine, Texas. Each balloon flight carried 37 standard solar cells for calibration above 99.5% of the earth's atmosphere. The solar cells were assembled into standard modules with appropriate resistors to load each cell at short-circuit current. In turn, each standardized module was mounted at the apex of the balloon on a sun tracker which automatically maintained normal incidence to the sun within ±1.0 deg. The balloons were launched to reach a float altitude of approximately 36.6 km (120,000 ft) two hours before solar noon and remain at float altitude for two hours beyond solar noon. Telemetered calibration data on each standard solar cell was collected during the float period and recorded on magnetic tape.

The magnetic tape was subsequently returned to JPL for data reduction and analysis. At the end of each float period the solar cell payload was separated from the balloon by radio command and descended via parachute to a ground recovery crew. Standard solar cells calibrated and recovered in this manner are used as primary intensity reference standards in solar simulators and in terrestrial sunlight for evaluating the performance of other solar cells and solar arrays with similar spectral response characteristics. This is now the most widely accepted technique for developing space standard solar cells in the United States.

Results of the 1973 NASA/JPL Balloon Flight Solar Cell Calibration Program

I. Introduction

For well over a decade, the primary source of electrical power for unmanned spacecraft and, more recently, for the manned Skylab, has been the direct conversion of solar energy through the use of solar cells. It is essential to the design of an array capable of meeting spacecraft requirements that the in-flight power output from these cells be accurately predictable from measurements previously made from either solar simulators or terrestrial sunlight. Since the short-circuit current of a solar cell is directly proportional to solar intensity, at least over a limited range, a calibrated solar cell may be obtained by accurately measuring its short-circuit current in a reference light source. For this purpose, the reference light source is extraterrestrial sunlight at a known earth–sun distance. To fill the need for accurately calibrated solar cells, JPL has established this solar cell calibration program using high-altitude balloon flights.

The altitude selected for the 1973/spring 1974 series of balloon flights was 36.6 km (120 kft). This choice was based on prior experience and was expected to eliminate, as much as possible, the effects of solar radiation absorption by the earth's atmosphere. When the spectral response of a majority of the solar cells (0.4 to 1.2 μm) is taken into consideration, the solar radiation at 36.6 km is essentially that of space sunlight. Table 1 shows the attenuation of solar radiation by the earth's atmosphere as a function of pressure and altitude over discrete wavelength regions throughout the solar spectrum (Ref. 1).

II. Use of Standard Solar Cells

Standard solar cells, calibrated by means of high-altitude balloon flights, are maintained and provided as a service to the photovoltaic community at large for flight and advanced development programs. The standards can be used in either of two ways.

(1) When used with artificial light sources, the standard cell is placed in the light beam and the intensity is adjusted until the output of the standard cell is equivalent to the 1 AU value or to any desired ratio of the calibrated value. The temperature of the standard cell is held constant at the standard temperature of 301.15 K (28°C). Once the intensity of the artificial light source has been set, the cells and/or panel that is to be measured is placed in the light beam and their parameters are then measured.

(2) When used as a calibration standard in terrestrial sunlight, the standard cell is placed in the same field of view as the solar cells or solar array being

Table 1. Attenuation of solar radiation by the earth's atmosphere (from Ref. 1)

<table>
<tr><th rowspan="2">Pressure, mbar[b]</th><th colspan="3">Altitude[a]</th><th colspan="9">Wavelength regions, μm</th><th rowspan="2">Altitude, km</th><th rowspan="2">IUGG[c]</th></tr>
<tr><th>Miles</th><th>10^3 feet</th><th>Kilometers</th><th>0.12 to 0.20</th><th>0.20 to 0.29</th><th>0.29 to 0.32</th><th>0.32 to 0.35</th><th>0.35 to 0.55</th><th>0.55 to 0.9</th><th>0.9 to 2.5</th><th>2.5 to 7</th><th>7 to 20</th></tr>
<tr><td>0.2</td><td>37</td><td>200</td><td>60</td><td>O_2 absorbs almost completely.</td><td colspan="8" rowspan="2">Solar irradiation intensity approximates extra atmospheric. Attenuation by scattering increases markedly toward shorter wavelengths.</td><td>Above 60</td><td rowspan="2">110 km
CHEMOSPHERE</td></tr>
<tr><td>7.5</td><td>20</td><td>108</td><td>33</td><td></td><td>(0.20 to 0.21 μm, absorption by O_2) Absorption by O_3 appreciable.</td><td>O_3 absorption not important.</td><td colspan="3"></td><td>Energy small</td><td>Energy very small</td><td>60 to 33</td></tr>
<tr><td>227</td><td>6.8</td><td>36</td><td>11</td><td></td><td>No radiation penetrates below about 11 km.</td><td>O_3 absorption attenuates more than loss by scattering.</td><td>O_3 absorption significantly attenuates radiation.</td><td>Irradiation diminished mostly by scattering by permanent gases in atmosphere.</td><td colspan="2" rowspan="2">H_2O responsible for major absorption; CO_2 absorbs slightly at 2 μm. Water vapor (or ice crystals) found up to about 70,000 feet.</td><td rowspan="3"></td><td>Strong O_3 absorption at 9.6 μm. Strong CO_2 absorption 12-17 μm.</td><td>33 to 11</td><td>20 km
STRATOSPHERE</td></tr>
<tr><td>795</td><td>1.2</td><td>6.6</td><td>2</td><td></td><td></td><td></td><td colspan="2">Highly variable dust, haze (H_2O), and smoke responsible for attenuation in regions 0.32 to 0.7 μm.</td><td>Energy transmitted with small loss down to 2 km.</td><td>Energy penetrates to sea level only through "windows" at approximately 1.2, 1.6, and 2.2 μm.</td><td>No significant penetration below 2 km, except in "windows" at approximately 3.8 and 4.9 μm.</td><td>Energy transmitted with moderate loss. Many absorption bands due to atmospheric gases.</td><td>11 to 2</td><td>11 km
TROPOSPHERE</td></tr>
<tr><td>1013</td><td colspan="3">Sea level</td><td></td><td></td><td>Appreciable penetration through "clear" atmosphere to sea level.
About 7%
About 30%</td><td>Penetration through "clear" atmosphere to sea level about 40%.</td><td colspan="3">Dust may rise to more than 4 kilometers.</td><td></td><td></td><td></td><td>2 to sea level</td><td>0 km</td></tr>
</table>

[a] NASA/JPL balloon flight program altitude = 36.6 km (120 kft).
[b] One mbar = 100 N/m^2.
[c] Nomenclature recommended by International Union of Geodesy and Geophysics (IUGG).

measured. Provisions should be made to maintain the standard cell at the standard temperature. If this is not practical, then the temperature of the standard cell must be measured and the output value corrected through application of the temperature coefficient. The output value of the standard solar cell is used to determine the incident solar radiation on the photovoltaic devices under test by direct ratio.

III. Balloon Flight Payloads

Payloads for the 1973/spring 1974 series of balloon flights comprised many types and configurations of solar cells. The solar cell packages were supplied by the organizations who participated in these series of flights (see Table 2).

To ensure compatibility with mechanical and electrical requirements of the balloon flight system, all packages were fabricated in accordance with the JPL Procedure for Balloon Flight Solar Cell Modules (Ref. 2). This procedure delineates physical size, mounting hole dimensions, dielectric insulation, and load resistor values in addition to material selection and assembly techniques.

The modules were shipped to JPL on or before a prescribed date for general workmanship and mechanical tolerances inspection. The modules were then given a preflight calibration measurement under the JPL X-25L Spectrolab Solar Simulator. This calibration served to correlate data supplied by the various organizations, taken with their own solar simulators and using their own calibration techniques. In general, correlation between the different organizations and the JPL Solar Simulator held to within ±2%. However, solar cells such as "Violet" and "Helios," which have enhanced spectral response characteristics in the shorter wavelength regions, exhibited values of only slight disagreement of approximately 1.5% between the JPL Solar Simulator and the resultant balloon flights.

Differences in correlation between the different participating organizations are explained by the use of different light sources, operation and maintenance of spectral tolerance, different standard solar cells used to establish light intensity, and measurement error. The Jet Propulsion Laboratory employs close-filtered xenon light sources (X25L and X25 Mark II Spectrolab Solar Simulators) which approximate space sunlight. Most organizations now employ this same type of solar simulator although, in the past, tungsten operated at 2800 K and carbon arc light sources have been used (Ref. 3).

The solar cell modules furnished by the organizations listed in Table 2 were divided into four separate payloads. Each payload is described separately in the latter sections of this report.

IV. Balloon Flight Performance

A. Flight 73-0 (789-P) and Flight 73-X (801-PT)

The initial attempt to launch a solar cell payload after a three-year interval was unsuccessful. On November 16, 1973, a launch failure inflicted serious damage to the sun tracker and to the solar cell payload. In the event solar cell modules are damaged, the JPL solar cell calibration program plan calls for spare modules to be on hand. And although many modules were damaged as a result of the launch failure, spare solar cell modules of the same type were available for replacement and were calibrated on subsequent flights.

The failure was analyzed, the top-mounted payload redesigned, and the launch technique improved. On January 7, 1974, a test flight (73-X) using dummy payloads was successful and seemed to prove that design changes were adequate.

B. Flight 73-1 (809-P)

Balloon flight 73-1, with solar cell modules mounted on the top payload, was successfully launched at 0823 CDT on February 16, 1974. The top payload weight was approximately 30 kg. A Raven 0.0254-mm tow balloon was used to help support the payload during launch. The launch, ascent, and float period were uneventful. Float altitude varied between 35,966 and 36,271 m. The flight was terminated at 1447 CDT, according to the aircraft radio communications log record book. Time of impact was not determined precisely because of nonreceipt of the radio beacon signal and lack of visual sighting. Impact was 12.8 km northeast of Groesbeck, Texas.

A preliminary investigation indicated that the parachute for the payload may not have been fully deployed during the descent. It appeared that the risers from one panel of the chute had wrapped around the other risers. Also, the parachute cords from the risers to the payload were tightly twisted and intertwined. There was some reason to suspect that the chute was turned inside out during its descent. The question appeared to be one of chute design: why did the chute perform satisfactorily on the experimental test flight (73-X) but not on the scientific flight? The only explanation given is the difference in weight of 6.4 kg. Thus it was recommended that, in the future, before using any new gear for the first time, every

Table 2. Solar cell module distribution and participating organizations for 1973/spring 1974 series of balloon flights

Telemetry channel	Flight 73-1/ organization	Flight 73-2/ organization	Flight 73-3/ organization	Flight 73-4/organization	
1	Goddard 73-012	Goddard 73-011A	Goddard 73-013	Goddard 73-015	Scheduled
2	Lewis 73-045	Lewis 73-046[b]	Goddard 73-014	Goddard 73-012A	Makeup
3	Lewis 73-048	Lewis 73-044	Lewis 73-04[illegible]	Lewis 73-051	Scheduled
4	LSMC 73-036	HAC 73-065	LSMC 73-037	Lewis 73-053	Scheduled
5	HAC 73-062	HAC 73-069	HAC 73-063	Lewis 73-047	Makeup
6	HAC 73-092	HAC 73-070	HAC 73-075	HAC 73-064	Scheduled
7	HAC 73-094	HAC 73-087	HAC 73-076	HAC 73-085	Scheduled
8	HAC 73-099	HAC 73-088	HAC 73-079	HAC 73-086	Scheduled
9	HAC 73-100	CRL 73-104	HAC 73-080	HAC 73-095	Scheduled
10	COMSAT 73-115	COMSAT 73-114	CRL 73-102	HAC 73-096	Scheduled
11	HEK 73-121	ESTEC 73-134	ESTEC 73-142[c]	HAC 73-066	Makeup
12	ESTEC 73-131N	Marshall 73-031	ESTEC 73-143[c]	HAC 73-090	Makeup
13	ESTEC 73-133	Marshall 73-033	RCA 73-164	HAC 73-091	Makeup
14	TRW 73-161[a]	JPL 73-001	Marshall 73-032	HAC 73-093	Makeup
15	JPL 73-007	JPL 73-002	JPL 73-153	HAC 73-099S	Makeup
16	JPL 73-008	JPL 73-003	JPL 73-154	CRL 73-103	Scheduled
17	JPL 73-009	JPL 73-004	JPL 73-155	HEK 73-123	Scheduled
18	JPL 73-010	JPL 73-005	JPL 73-156	HEK 73-122	Makeup
19	JPL 73-151	JPL 73-006	JPL 73-157	ESTEC 73-136	Scheduled
20	JPL 73-152	JPL BFS401	JPL 73-158	ESTEC 73-137	Makeup
21	JPL 73-X	JPL BFS403	JPL 73-159	ESTEC 73-141	Makeup
22	JPL BFS110A	JPL BFS404	JPL 73-160	COMSAT 73-111	Makeup
23	JPL BFS110B	JPL BFS406	JPL 73-173	Marshall 73-034	Scheduled
24	JPL BFS112A	JPL BFS501	JPL BFS113A	TRW 73-180	Makeup
25	JPL BFS112B	JPL BFS502	JPL BFS113B	JPL 73-181	Scheduled
26	JPL BFS307	JPL SM3-11	JPL BFS115A	JPL 73-171	
27	JPL BFS309	JPL SM3-15	JPL BFS115B	JPL 73-172	
28	JPL BFS402	JPL BFS02A	JPL BFS506	JPL 73-176 Cu temp	
29	JPL BFS503	JPL BFS02B	JPL BFS507	JPL 73-183 Al temp	
30	JPL BFS601	JPL BFS405	JPL BFS508	JPL BFS7007	
31	JPL BFS518A	JPL BFS517A	JPL BFS520A	JPL BFS7010	
32	JPL BFS518B	JPL BFS517B	JPL BFS520B	JPL BFS7011	
33	JPL BFS518C	JPL BFS517C	JPL BFS520C	JPL BFS604	
34	JPL BFS7002	JPL BFS7002	JPL BFS7002	JPL BFS605	
35	JPL BFS505	JPL BFS505	JPL BFS505	JPL BFS505	
36	JPL BFS17A	JPL BFS17A	JPL BFS17A	JPL BFS17A	
37	JPL BFS17B	JPL BFS17B	JPL BFS17B	JPL BFS17B	
38	On-Sun	On-Sun	On-Sun	On-Sun indicator	

[a] Postflight analysis and test indicate that the positive terminal of this cell was shorted to its substrate and caused ground loop in telemetry.
[b] This solar cell module replaced 73-042, which was found to be shorted to ground during preflight checkout.
[c] Solar cell module replaced with spare due to flight plan modification and/or found to be shorted during preflight checkout.

Organization Code:

GODDARD	NASA Goddard Space Flight Center
LEWIS	NASA Lewis Research Center
MARSHALL	NASA Marshall Space Flight Center
HAC	Hughes Aircraft Co.
TRW	TRW Inc.
HEK	Heliotek/Spectrolab
LSMC	Lockheed Missiles and Space Co.
COMSAT	Communications Satellite Corp.
RCA	Radio Corporation of America
CRL	Centralab Semiconductors
ESTEC	European Space Research Organization, European Space Research and Technology Centre
JPL	Jet Propulsion Laboratory/Caltech

reasonable inquiry should be made to determine whether any problems in its use have ever been encountered. Insofar as the radio beacon signal and top payload are of concern, it was recommended that primary effort for reception and tracking be directed toward the scientific payload rather than the bottom payload. It was the opinion of the critique board that, if the radio beacon had been the primary signal monitored, it could have been more readily determined whether the scientific payload had impacted much earlier than planned and, therefore, the payload could have been located much sooner.

The top payload was lost for approximately one week and was finally found on the morning of February 25, 1974, near Groesbeck, Texas. It had come down in an open grassy field. The parachute had rotated during descent, and the shroud lines were wound around each other as indicated earlier. When impact occurred, the parachute fell inside the aluminum-hoop assembly, being pulled in by the twisted lines, and only a small area of the two-colored parachute was visible. The sun tracker was severely damaged. The solar cell payload had tipped over toward the north and turned upside down. The reflection shield assisted in preventing damage to the cells. The solar cells were thus protected from direct sunlight and also from direct rainfall, although some splashing was evident on a few modules. Temperatures during the time the payload was missing never approached freezing. After recovery of the damaged electronics, sun tracker, and solar cell modules, the latter two items, including the test-data tape, were returned to JPL for repair and for processing of test data.

Figure 1 shows the relative locations of the solar cell modules; a corresponding photograph of the payload is shown in Fig. 2.

C. Flight 73-2 (814-P)

Balloon flight 73-2, with solar cell modules mounted on the top payload, was successfully launched at 0842 CDT on April 5, 1974. All electronic systems operated as anticipated and good data was obtained. The flight was terminated slightly earlier than planned because the balloon was heading toward Baton Rouge, Louisiana. At termination, the parachute for the top-mounted payload apparently failed to deploy properly, resulting in a much higher descent rate and a more severe impact than normal.

Fortunately, the top payload landed in the relatively soft marsh area outside Baton Rouge. Although the top payload solar cells were subjected to this abnormal landing and mud, subsequent cleaning of the sun tracker, electronic equipment, and solar cell modules indicated that only one cell had been damaged (73-046). In addition, the cover glasses of seven JPL solar cell modules had been chipped. Subsequently, electrical performance measurements made of the electronics, sun tracker, and solar cell modules indicated that only minor damage had occurred.

As a result, the magnetic data tape was processed through the JPL computer, and copies of the results were sent to the participating organizations together with their solar cell modules. A diagram of the various solar cell modules showing their relative locations on the sun tracker for this flight (73-2) is shown in Fig. 3. A corresponding photograph of the payload for this flight is shown in Fig. 4.

D. Experimental Test Flight 73-XX (818-P)

A second experimental test balloon flight, 73-XX, was launched on April 1[illegible] 1974, and a successful recovery was made. The primary purposes of this test flight were to check out the modifications made to the recovery radio beacon and the deployment of the modified descent parachute. The flight altitude attained during the flight was approximately 36,881 m; it was maintained for one hour. The descent time was about 36 min to touchdown. The descent rate was calculated to be about 6.4 m/s, which is indicated as being a normal descent rate by parachute. It was also interesting to note that the top payload is subjected to about 3 g when the chute deploys. As a result of this successful operation, the third of the planned series of four flights was once again resumed.

E. Flight 73-3 (819-P)

Balloon flight 73-3, with solar cell modules mounted on the top payload, was successfully launched at 0721 CDT on April 23, 1974. All electronic systems operated as anticipated and good data was obtained. A minor problem did occur, however, just prior to termination of flight at float altitude. The sun tracker photodiodes used to detect elevation alignment to the sun were apparently set at too great a sensitivity. This caused the sun tracker to go into an oscillation mode near termination of the mission. Fortunately, good data was received prior to this event and was returned to JPL for data reduction and processing. The recovery phase of the flight to touchdown was uneventful; the payload was recovered on the same day (April 23).

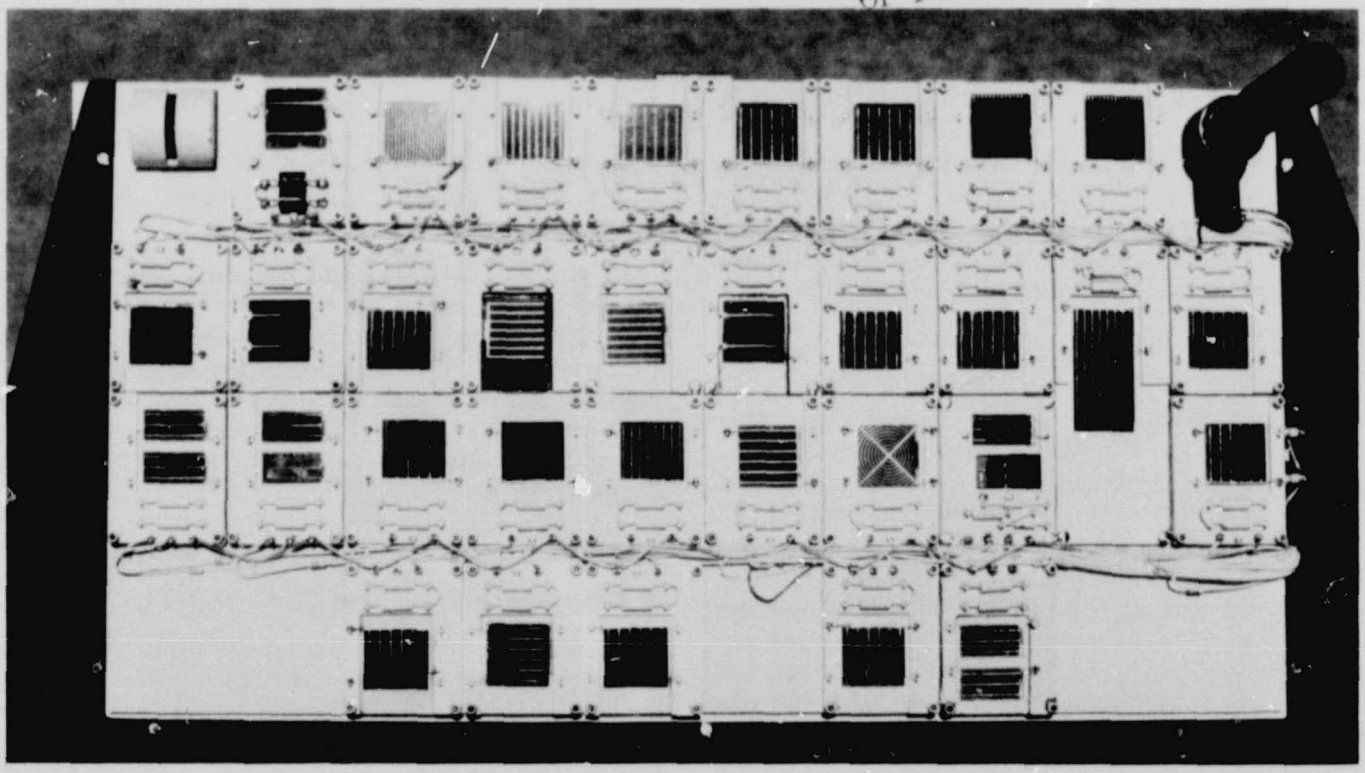

Fig. 1. Solar cell payload for balloon flight 73-1

	GODDARD 73-012 (3)	LEWIS 73-045 (4)	LEWIS 73-048 (5)	HUGHES 73-062 (6)	HUGHES 73-092 (8)	HUGHES 73-094 (9)	HUGHES 73-099 (10)	HUGHES 73-100 (11)	ON SUN
JPL BFS-503 (12)	COMSAT 73-115 (13)	HEK 73-121 (15)	ESTEC 73-131N (16)	ESTEC 73-133 (17)	TRW 73-161 (19)	JPL 73-007 (20)	JPL 73-008 (22)	LOCKHEED 73-036 (23) (2 X 4)	JPL 73-009 (24)
JPL BFS-110 A (25) B (26)	JPL BFS-112 A (27) B (29)	JPL 73-010 (30)	JPL 73-151 (31)	JPL 73-152 (32)	JPL BSF-7002 (33) TEMP. (18) T_2	JPL 73-X (36)	JPL BFS-518 A (37) B (38) C (39)		JPL BFS-505 (40) TEMP. (34) T_3
BLANK	BLANK	JPL BFS-307 (41)	JPL BFS-309 (43)	JPL BFS-402 (44)	BLANK	JPL BFS-601 (45)	JPL BFS-17 A (46) B (47)	BLANK	BLANK

O INDICATES CHANNEL NO.

Fig. 2. Solar cell calibration module location chart, balloon flight 73-1

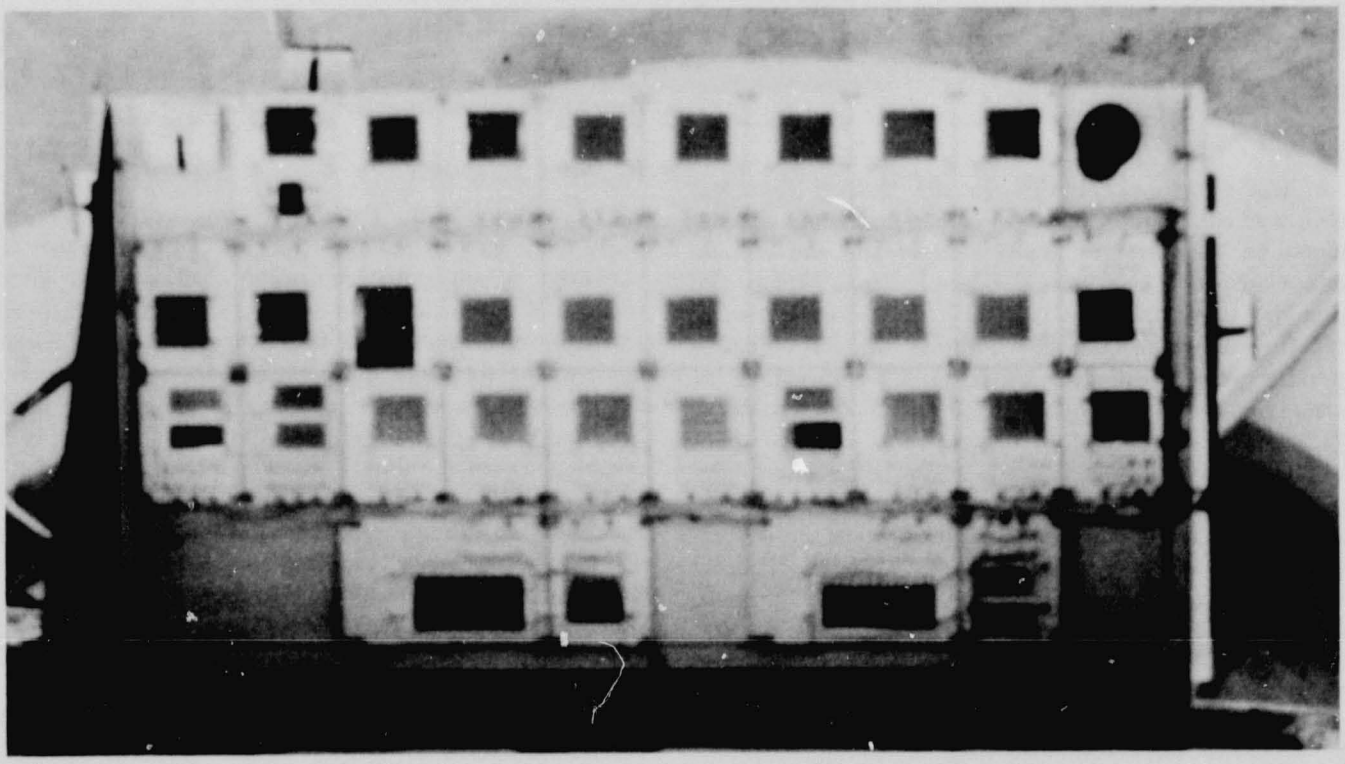

Fig. 3. Solar cell payload for balloon flight 73-2

	GODDARD 73-011A (3)	LEWIS 73-046 (4)	LEWIS 73-044 (5)	HUGHES 73-065 (6)	HUGHES 73-069 (8)	HUGHES 73-070 (9)	HUGHES 73-087 (10)	HUGHES 73-088 (11)	
CENTRA-LAB 73-104 (12)	COMSAT 73-114 (13)	ESTEC 73-134 (15)	JPL 73-001 (16)	JPL 73-002 (17)	JPL 73-003 (19)	JPL 73-004 (20)	JPL 73-005 (22)	JPL 73-006 (23)	JPL BFS-401 (24)
JPL 1A3 -11 (25) -15 (26)	JPL BFS-02 A (27) B (29)	JPL BFS-403 (30)	JPL BFS-404 (31)	JPL BFS-405 (32)	JPL BSF-7002 (33) T_2 (18)	JPL BFS-517 A (36) B (37) C (38)	JPL BFS-406 (39)	JPL BFS-501 (40)	JPL BFS-505 (41) T_3 (84)
BLANK	BLANK		MARSHALL 73-031 (2 X 4) (43)	JPL BFS-502 (44)	BLANK		MARSHALL 73-033 (2 X 4) (45)	JPL BFS-17 A (46) B (47)	BLANK

○ INDICATES PCM TELEMETRY CHANNEL NO.

Fig. 4. Module location for balloon flight 73-2

Figure 5 shows the various solar cell modules and their relative locations on the sun tracker for this flight (73-3). A photograph of the solar cell modules is shown in Fig. 6.

F. Flight 73-4 (825-P)

A final system check through the balloon electrical cable was completed May 6. Weather conditions for the launch on May 8 were nearly perfect and the balloon system ascended in a normal manner. From launch, the telemetry transmitter was on, and it functioned perfectly until the balloon reached float altitude, when it began to operate intermittently. In order to take advantage of normal light wind conditions around sunrise, launch was at 0715 CDT, and therefore the balloon reached float altitude about 0930 CDT, several hours before solar noon at 1300. Because of the transmitter problem and the early hour, the sun tracker was not turned on when the balloon reached float. At first, it was suspected that the difficulty was in the receiving antenna, since the NSBF had never before experienced an inflight transmitter failure. Several attempts to correct the transmitter malfunction were made by commanding the transmitter off and then on again, and by commanding the transmitter off for a 15-min cooling period and then turning it on, but no improvement was apparent. Basically, the transmitter was off about 90% of the time, coming on in short bursts of 2 or 3 s.

It was decided to turn the sun tracker on and have it locked on the sun, with everything ready in the event the transmitter stayed on for a significant period. Toward solar noon, it was observed that the transmitter had remained on for periods of several seconds and sometimes nearly a minute. While the transmitter was on, it was observed that the On-Sun indicator registered an on-sun condition each time, thus indicating that the sun tracker was functioning properly.

Only minimum data was recorded on tape, but it was believed that it would be sufficient for reduction and analysis. Backup data was recorded on teletype printout. Flight termination was as planned and the parachute descent of the sun tracker and solar cell payload was without incident and marked the first normal recovery of the top-mounted package. The sun tracker was only slightly damaged and the solar cell payload was found to be in perfect condition.

A diagram of the various solar cell modules, showing their relative locations on the sun tracker for this flight (73-4), is shown in Fig. 7. Figure 8 is a corresponding photograph of the payload.

V. Discussion of Solar Cell Calibration Data

A. Flight 73-0 Data

Owing to the balloon failure at launch of flight 73-0, no data was obtained from the payload.

B. Flight 73-1 Data

Data obtained from the solar cell payload was continuously recorded from the time the sun tracker was activated by telemetry command until the end of the required float period. Data taken prior to the float period is not normally used in the final data reduction procedure, because the solar cell temperatures are changing rapidly and the sun tracker has difficulty in maintaining on-sun lock due to a higher degree of balloon rotation during the ascent phase of the flight. Data recorded from flight 73-1 is questionable because of the synergistic effects caused by reflection from the protective hoop around the sun tracker and a shorted solar cell module, 73-161. The latter problem further complicated matters by producing a ground loop, causing an interference with the telemetry system. This problem was earlier thought to be caused by RF interference between the radio beacon and telemetry system. As a result of the above uncertainties, the calibration data is not included in this report for flight 73-1. Instead, a series of cross correlation measurements is suggested on these cells against cells calibrated on subsequent flights (73-3 through 73-4).

C. Flight 73-2 Data

Data obtained from the solar cell payload was continuously recorded in a manner similar to that of flight 73-1. Good data was obtained, yielding a high degree of confidence. Subsequent processing of the flight data through the JPL computer program confirmed the results obtained on ground teletype. Table 3 is a summary of the results of flight 73-2. The modules are listed by serial number and cross referenced to the telemetry channel number. The temperature and intensity adjusted average in millivolts is the computer-corrected solar cell output average of approximately 100 data points. This value has been corrected to 1 AU (average earth–sun distance) and from the cell flight temperature to 28°C if a temperature coefficient value was supplied by the participant. If the cell temperature coefficient was unknown, then the value listed is only corrected to the 1 AU intensity. The actual average temperature during the period data was taken is listed on the table as a footnote. The 95% confidence limits and standard deviation are listed for each cell in separate columns. In addition, the results obtained from the JPL solar simulator are shown in Table 4. As mentioned earlier, this table shows the results of

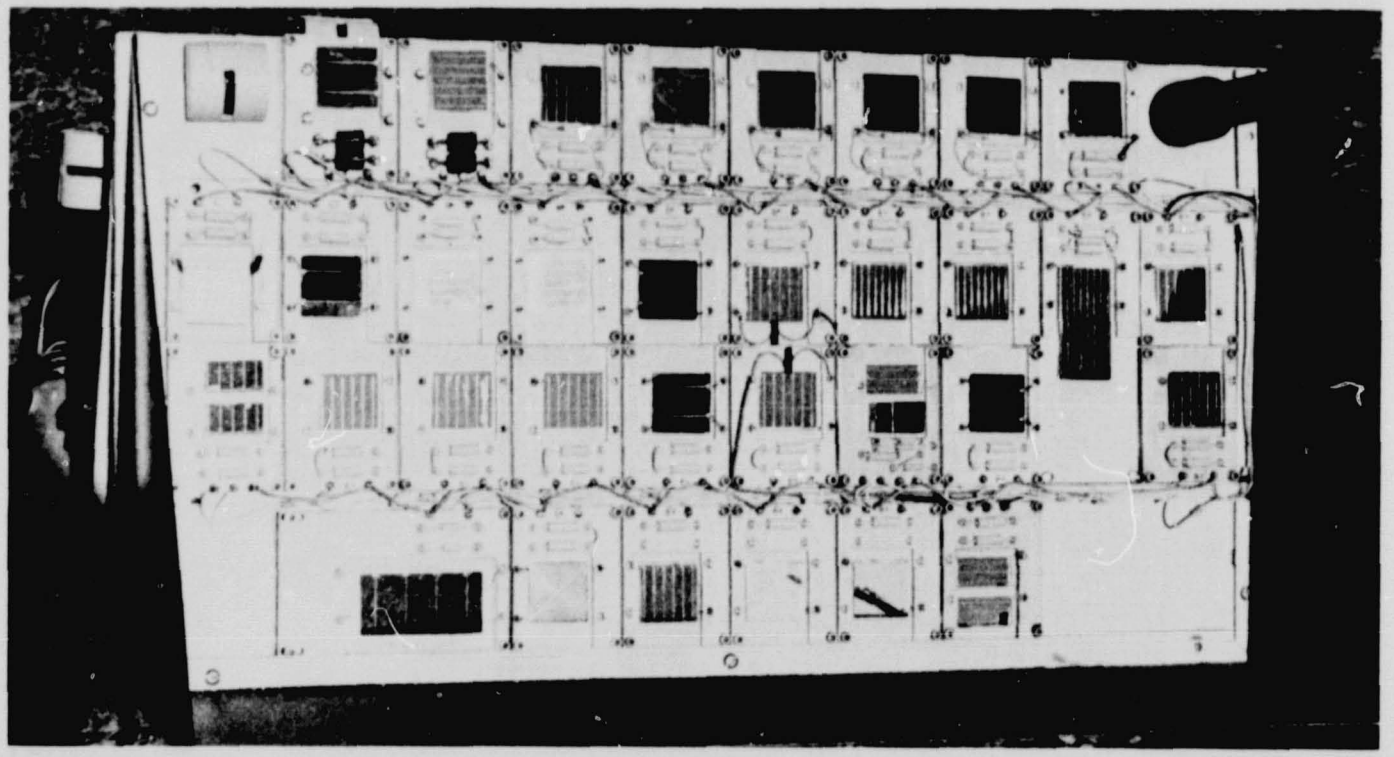

Fig. 5. Solar cell payload for balloon flight 73-3

	GODDARD 73-013 (3)	GODDARD 73-014 (4)	HUGHES 73-063 (5)	HUGHES 73-075 (6)	HUGHES 73-076 (8)	HUGHES 73-079 (9)	HUGHES 73-080 (10)	LEWIS 73-049 (11)
LEWIS 73-052 (12)	CRL 73-102 (13)	ESTEC 73-142 (15)	ESTEC 73-143 (16)	RCA 73-164 (17)	JPL 73-175 (19) CU T_2 (18)	JPL 73-153 (20)	JPL 73-154 (22)	LOCKHEED 73-037 (23)	JPL 73-155 (24)
JPL BFS-115 A (25) B (26)	JPL 73-156 (27)	JPL 73-157 (30)	JPL 73-158 (31)	JPL 73-159 (32)	JPL 73-182 (33) AL T_3 (34)	JPL BFS-520 A (36) B (37) C (38)	JPL 73-160 (39)	2 X 4 73-037	JPL BFS-505 (40)
BLANK		MARSHALL 73-032 (2 X 4) (29)	JPL 73-173 (41)	JPL BFS-506 (43)	JPL BFS-507 (44)	JPL BFS-508 (45)	JPL BFS-17 A (46) B (47)	BLANK	BLANK

O INDICATES PCM TELEMETRY CHANNEL NO.

Fig. 6. Module location for balloon flight 73-3

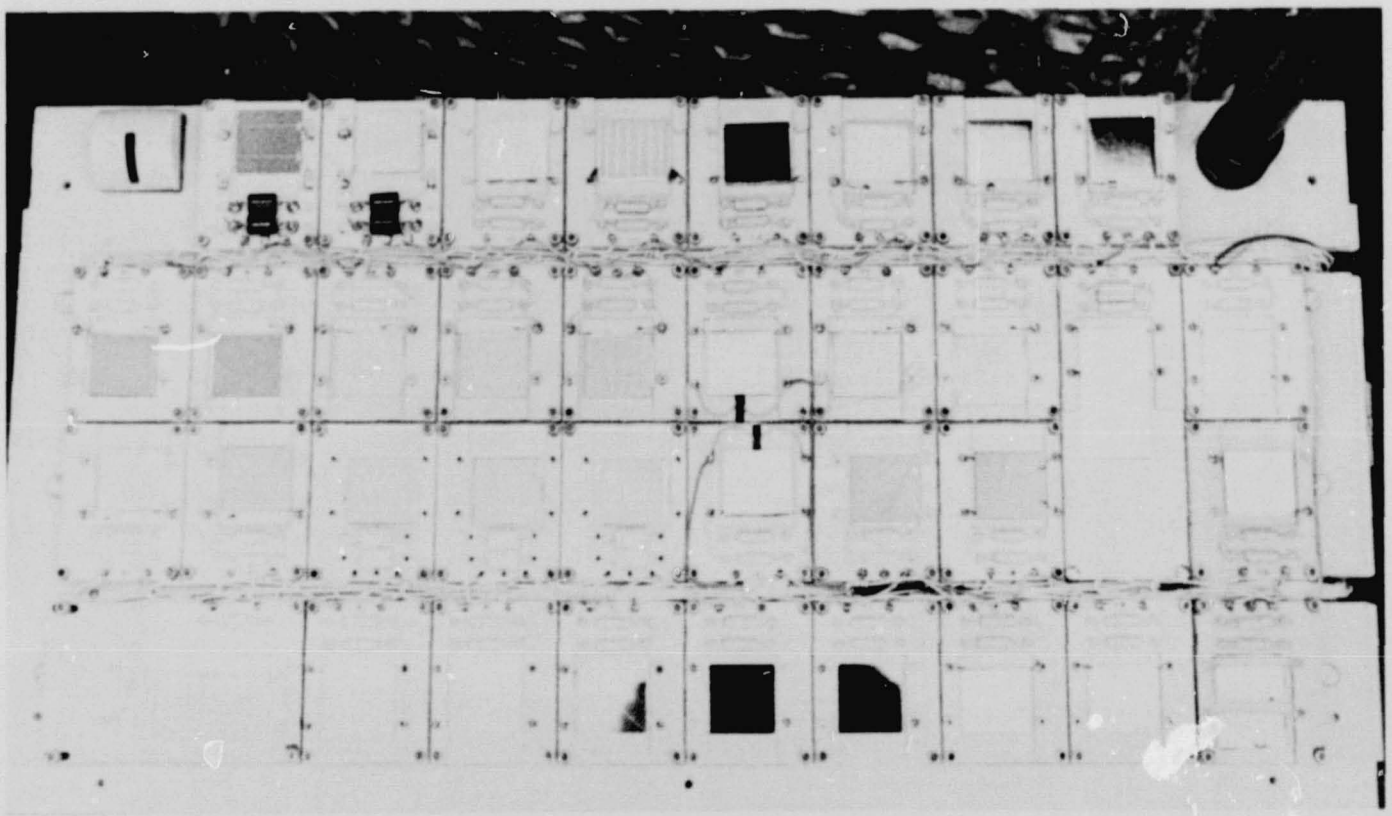

Fig. 7. Solar cell payload for balloon flight 73-4

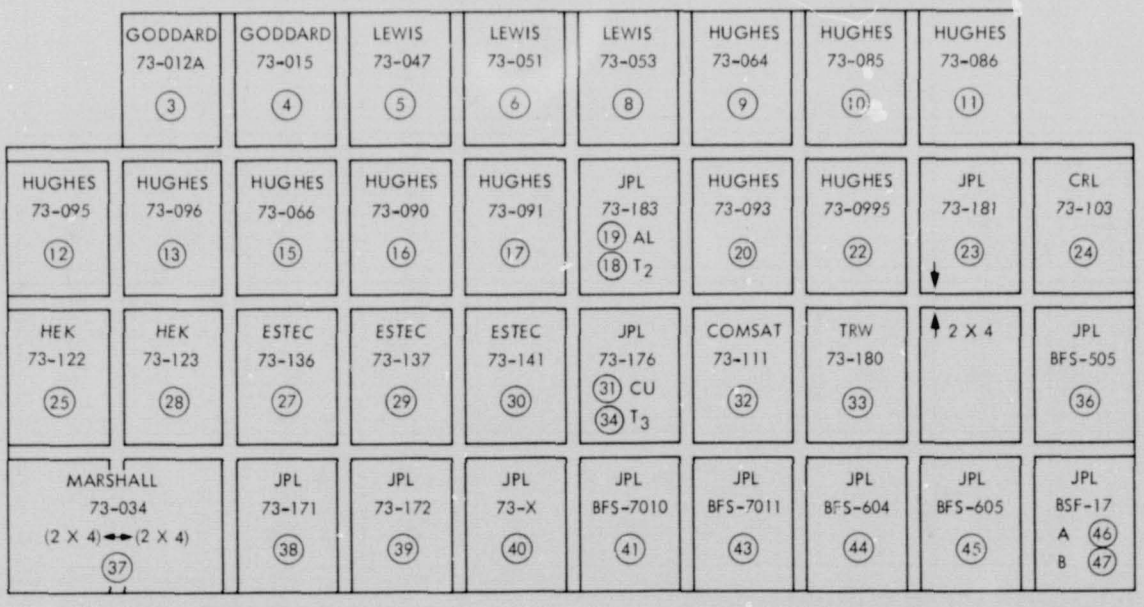

Fig. 8. Module location for balloon flight 73-4

measurements obtained under air-mass-zero solar simulation before and after the flight (preflight vs postflight), and a comparison is made between the preflight simulator data and resultant flight data. Again, these comparisons are made only on cells in which temperature coefficients have been provided.

D. Flight 73-3 Data

Except for minor sun tracker oscillations encountered near termination at float altitude, the flight data observed from ground station telemetry looked good, and the magnetic tape comprising the data was sent to JPL for computer processing. The solar cell standards were also returned to JPL for postflight solar simulator measurements, inspection, and analysis. The results of flight 73-3 are shown in Table 5. The column headings and data organization in Table 5 are similar to those of Table 3, described earlier. In addition, the results obtained from the JPL solar simulator are shown in Table 6. As mentioned earlier, this table shows the results of measurements obtained under air-mass-zero solar simulation before and after the flight (preflight vs postflight), and a comparison is made between the preflight simulator data and resultant flight data. Again, these comparisons are made only on cells in which temperature coefficients have been provided.

E. Flight 73-4 Data

Major changes were made to the selection of the solar cell modules received from the various participating organizations. These changes included requests obtained from various organizations regarding the replacement of solar cell modules. Changes were also made by JPL to accommodate additional flights of spare solar cell modules similar to those flown on flight 73-1. These changes were made after it was discovered that module 73-161, flown on 73-1, was shorted to telemetry ground, causing a ground loop in the system. Solar cell data was further complicated by reflections from the aluminum-hoop assembly which protects the sun tracker during landing. Additional checkout procedures, beginning with flight 73-2, were incorporated during the ground testing operations. Subsequent measurements made of the remaining solar cell modules indicated that modules 73-042, 73-161, 73-162, and 73-132 were also shorted to the substrate. Because of this shorted condition, these spare modules were not flown.

Balloon flight 73-4 was successfully launched at 0715 CDT, May 8, 1974, and recovered on the same day. Good data was obtained in spite of an intermittent transmitter anomaly which occurred during this flight. While the transmitter was on, the On-Sun indicator registered an on-sun condition each time, thus indicating that the sun tracker was functioning properly. Although only a minimum amount of data was recorded on the tape, it was sufficient for processing on the JPL computer. Backup data received from ground telemetry teletype was also obtained for analysis. A summary of the results of this flight is shown in Table 7. Table 8 shows the results of the solar simulator measurements obtained under air-mass-zero solar simulation in comparison with flight data.

VI. Balloon Flight System

The main components of the balloon flight system are (a) the apex-mounted hoop assembly which contains the primary payload, the telemetry system and the recovery system, (b) the balloon, and (c) the lower payload. This configuration differs from that employed in past calibration programs and is described in the following sections.

A. The Apex-Mounted Hoop Assembly

1. General description. The aluminum-tubular hoop assembly shown in Fig. 9 is used as a mounting platform for the primary payload and several other apex-mounted components. The hoop assembly, with appropriately placed styrofoam crush pads, serves the following functions:

(1) Permits the top-mounted payload to "float" atop the helium bubble and minimizes billowing of balloon material around the top payload.

(2) Serves as the mounting surface to the balloon's top end fitting.

(3) Provides a convenient point for attachment of the tow balloon.

(4) Acts as a shock damper to protect and minimize damage to the top payload when touchdown occurs.

The complete apex-mounted hoop assembly as flown weighs approximately 31.8 kg and descends as a unit by parachute at flight termination.

2. The experimental package. The elements of the experimental package are described below.

a. Sun tracker. Using photodiodes as sensors, the sun tracker, shown in Fig. 10, is capable of orienting a solar cell payload toward the sun independent of balloon movements and is able to move in both elevation and azimuth to maintain an on-sun condition within ±1 deg. To verify that the sun tracker is actually pointing at the sun, an On-Sun indicator, which consists of a small,

Table 3. Summary of balloon flight 73-2 results

Module number	Channel number	Temperature intensity, adjusted average, mV (1 AU, 28°C)	95% confidence limits	Standard deviation
73-011A	3	79.22[a]	0.01303	0.06513
73-046	4	80.01[a]	0.01348	0.06742
73-044	5	57.84	0.01087	0.05436
73-065	6	75.83	0.01025	0.05125
73-069	8	76.59	0.01279	0.06396
73-070	9	76.99	0.01181	0.05903
73-087	10	79.04	0.01137	0.05685
73-088	11	80.55	0.00985	0.04924
73-104	12	80.39[a]	0.02118	0.10589
73-114	13	82.64	0.01435	0.07177
73-134	15	60.00	0.01477	0.07385
73-001	16	67.23	0.01859	0.09293
73-002	17	66.70	0.01155	0.05774
73-003	19	66.40	0.01263	0.06317
73-004	20	66.83	0.01886	0.09428
73-005	22	67.07	0.01073	0.05365
73-006	23	66.50	0.01263	0.06317
BFS-401	24	60.32	0.01608	0.08040
SM3-11	25	62.86	0.01214	0.06072
SM3-15	26	56.96	0.00969	0.04846
BFS-02A	27	63.89	0.01608	0.08040
BFS-02B	29	58.93	0.01470	0.07351
BFS-403	30	61.28	0.02292	0.11459
BFS-404	31	61.80	0.01421	0.07107
BFS-405	32	61.24	0.01781	0.08905
BFS-7002	33	65.29	0.01279	0.06396
BFS-517A	36	22.16	0.00991	0.04956
BFS-517B	37	22.36	0.01080	0.05401
BFS-517C	38	64.82	0.01491	0.07454
BFS-406	39	63.85	0.01407	0.07035
BFS-501	40	67.67	0.01137	0.05685
BFS-505	41	65.31	0.01378	0.06890
73-031	43	77.44[a]	0.02474	0.12371
BFS-502	44	59.94	0.02395	0.11976
73-033	45	63.69[a]	0.01803	0.09017
BFS-17A	46	60.37	0.01627	0.08134
BFS-17B	47	60.49	0.02197	0.10987

Average temperature at float altitude, 45.19°C.
Float altitude, approximately 36.6 km.
Launch date, Feb. 5, 1974.
[a]Channel for which no temperature coefficient was provided.

Table 4. Summary of balloon flight 73-2 results compared with solar simulator measurements

Organization code	Module number	AMO, solar simulator (1 AU, 28°C)		Comparison, solar simulator and flight		Comments, postflight
		Preflight, mV	Postflight, mV	Preflight vs postflight, %	Flight vs preflight, %	
Goddard	73-011A[a]	78.28	78.25	0.04		
Lewis	73-046[a]	78.84	64.53	18.15		Broken cell
Lewis	73-044	57.86	57.66	0.35	-0.03	
HAC	73-065	75.65	75.20	0.59	0.24	
HAC	73-069	76.82	76.55	0.35	-0.30	
HAC	73-070	76.90	76.74	0.21	0.12	
HAC	73-087	79.25	78.84	0.52	-0.26	
HAC	73-088	80.82	80.42	0.49	-0.33	
CRL	73-104[a]	80.28	79.50	0.97		
COMSAT	73-114	81.82	81.22	0.73	0.99	
ESTEC	73-134	59.96	59.92	0.07	0.07	
JPL	73-001	68.68	68.16	0.76	-2.16	
JPL	73-002	68.15	67.28	1.28	-2.17	
JPL	73-003	67.80	67.33	0.69	-2.11	
JPL	73-004	68.04	67.72	0.47	-1.81	
JPL	73-005	68.30	68.05	0.37	-1.84	
JPL	73-006	67.67	67.47	0.30	-1.76	
JPL	BFS-401	61.30	61.32	-0.03	-1.63	
JPL	SM3-11	62.00	58.30	5.97	1.37	
JPL	SM3-15	57.50	57.52	-0.03	-0.95	
JPL	BFS-02A	63.90	64.00	-0.16	-0.02	
JPL	BFS-02B	59.30	59.03	0.46	-0.62	
JPL	BFS-403	62.25	62.00	0.40	-1.58	Broken filter
JPL	BFS-404	62.75	62.50	0.40	-1.54	
JPL	BFS-405	62.14	61.79	0.56	-1.47	
JPL	BFS-7002	66.05	66.07	-0.03	-1.17	Filter chip
JPL	BFS-517A	22.03	21.57	2.09	0.56	
JPL	BFS-517B	23.22	21.93	5.56	-3.85	
JPL	BFS-517C	65.00	65.10	-0.15	-0.28	
JPL	BFS-406	65.35	65.04	0.47	-2.35	
JPL	BFS-501	68.10	68.04	0.09	-0.64	
JPL	BFS-505	66.10	66.17	-0.11	-1.21	
Marshall	73-031[a]	78.15	77.45	0.90		
JPL	BFS-502	60.50	60.50	0.00	-0.93	
Marshall	73-033[a]	65.17	63.75	2.18		
JPL	BFS-17A	60.17	60.60	-0.71	0.33	
JPL	BFS-17B	59.70	60.32	-1.04	1.30	

Average temperature at float altitude, 45.19°C.
Float altitude, approximately 36.6 km.
Launch date, Feb. 5, 1974.
[a]Channel for which no temperature coefficient was provided.

Table 5. Summary of balloon flight 73-3 results

Module number	Channel number	Temperature intensity, adjusted average, mV (1 AU, 28°C)	95% confidence limits	Standard deviation
73-013	3	83.10[a]	0.01101	0.05505
73-014	4	66.87[a]	0.00995	0.04975
73-063	5	75.18	0.01803	0.09017
73-075	6	82.48	0.02412	0.12060
73-076	8	80.89	0.01518	0.07588
73-079	9	77.88	0.01295	0.06475
73-080	10	76.62	0.00739	0.03693
73-049	11	75.08[a]	0.00943	0.04714
73-052	12	72.02[a]	0.01959	0.09796
73-102	13	80.27[a]	0.00636	0.03178
73-142	15	57.59	0.01124	0.05618
73-143	16	66.67	0.00910	0.04551
73-164	17	82.26[a]	0.01101	0.05505
73-175	19	67.81	0.00910	0.04551
73-153	20	74.84	0.00964	0.04820
73-154	22	75.73	0.02399	0.11997
73-037	23	73.48[a]	0.00348	0.01741
73-155	24	59.60	0.01583	0.07914
BFS-115A	25	57.62	0.01655	0.08273
BFS-115B	26	57.80	0.01314	0.06571
73-156	27	61.51	0.02005	0.10025
73-032	29	78.27[a]	0.01400	0.06999
73-157	30	64.42	0.00876	0.04381
73-158	31	65.52	0.02108	0.10541
73-159	32	79.28	0.02074	0.10372
73-182	33	68.37	0.00667	0.03333
BFS-520A	36	23.93	0.01771	0.08855
BFS-520B	37	23.20	0.00952	0.04761
BFS-520C	38	66.62	0.00995	0.04975
73-160	39	79.90	0.01143	0.07213
BFS-505	40	65.43	0.01054	0.05270
73-173	41	62.78	0.01231	0.06155
BFS-506	43	31.42	0.00948	0.04741
BFS-507	44	37.53	0.00964	0.04820
BFS-508	45	30.69[a]	0.01020	0.05100
BFS-17A	46	60.37	0.01363	0.06816
BFS-17B	47	60.67	0.01633	0.08165

Average temperature at float altitude, 54.25°C.
Float altitude, approximately 36.6 km.
Launch date, Apr. 23, 1974.
[a]Channel for which no temperature coefficient was provided.

Table 6. Summary of balloon flight 73-3 results compared with solar simulator measurements

Organization code	Module number	AMO, solar simulator (1 AU, 28°C)		Comparison, solar simulator and flight		Comments, postflight
		Preflight, mV	Postflight, mV	Preflight vs postflight, %	Flight vs preflight, %	
Goddard	73-013[a]	80.85	80.82	0.04		None
Goddard	73-014[a]	65.95	66.12	0.26		
HAC	73-063	75.00	74.96	0.05	0.24	
HAC	73-075	81.54	81.70	-0.20	1.14	
HAC	73-076	80.06	79.96	0.12	1.02	
HAC	73-079	77.46	77.15	0.40	0.54	
HAC	73-080	76.05	75.95	0.13	0.75	
Lewis	73-049[a]	73.88	73.58	0.41		
Lewis	73-052[a]	70.46	70.31	0.21		
CRL	73-102[a]	78.54	77.89	0.83		
ESTEC	73-142	57.50	56.69	1.41	0.16	
ESTEC	73-143	68.65	68.42	0.34	-2.97	
RCA	73-164[a]	81.55	80.38	1.43		
JPL	73-175	68.70	68.45	0.36	-1.31	
JPL	73-153	74.84	74.86	-0.03	0.00	
JPL	73-154	75.45	75.39	0.08	0.37	
LSMC	73-037[a]	72.86	73.39	-0.73		
JPL	73-155	60.40	60.87	-0.78	-1.34	
JPL	BFS-115A	57.68	57.86	-0.31	-0.11	
JPL	BFS-115B	57.90	58.36	-0.79	-0.17	
JPL	73-156	62.28	62.48	-0.32	-1.25	
Marshall	73-032[a]	78.15	77.68	0.60		
JPL	73-157	65.00	65.28	-0.43	-0.90	
JPL	73-158	67.90	66.02	2.77	-3.63	
JPL	73-159	79.70	79.20	0.63	-0.53	
JPL	73-182	69.30	68.89	0.59	-1.36	
JPL	BFS-520A	23.48	23.85	-1.58	1.89	
JPL	BFS-520B	23.75	23.08	2.82	-2.35	
JPL	BFS-520C	67.50	67.54	-0.06	-1.32	
JPL	73-160	80.18	79.52	0.82	-0.35	
JPL	BFS-505[b]					
JPL	73-173	63.65	63.94	-0.46	-1.39	
JPL	BFS-506	32.15	30.67	4.60	-2.34	
JPL	BFS-507	39.60	38.76	2.12	-5.52	
JPL	BFS-508[a]	32.25	31.19	3.29		
JPL	BFS-17A[b]					
JPL	BFS-17B[b]					

Average temperature at float altitude, 54.25°C.
Float altitude, approximately 36.6 km.
Launch date, Apr. 23, 1974.
[a]Channel for which no temperature coefficient was provided.
[b]Reference module; no post flight measurements made.

Table 7. Summary of balloon flight 73-4 results

Module number	Channel number	Temperature intensity, adjusted average, mV (1 AU, 28°C)	95% confidence limits	Standard deviation
73-012A	3	80.52[a]	0.01700	0.08498
73-015	4	68.10[a]	0.01333	0.06667
73-047	5	56.57[a]	0.02220	0.11101
73-051	6	69.32[a]	0.01206	0.06030
73-053	8	47.78[a]	0.01967	0.09834
73-064	9	74.14	0.01231	0.06155
73-085	10	79.27	0.02738	0.13688
73-086	11	78.37	0.01119	0.05596
73-095	12	65.95	0.01470	0.07351
73-096	13	67.13	0.01484	0.07420
73-066	15	75.16	0.01255	0.06276
73-090	16	79.69	0.01676	0.08379
73-091	17	75.83	0.02010	0.10050
73-183	19	67.51	0.01155	0.05774
73-093	20	75.32	0.02118	0.10589
73-0995	22	86.49	0.01463	0.07317
73-181	23	68.18	0.01035	0.05174
73-103	24	76.10[a]	0.01639	0.08196
73-122	25	74.52	0.01902	0.09508
73-123	26	81.48	0.02179	0.10894
73-136	27	58.70	0.02010	0.10050
73-137	29	57.88	0.02134	0.10672
73-141	30	68.53[a]	0.01869	0.09347
73-176	31	67.05	0.01896	0.09482
73-111	32	82.97	0.02704	0.13521
73-180	33	79.35[a]	0.01128	0.05641
BFS-505	36	65.37	0.02574	0.12871
73-034	37	66.86[a]	0.01896	0.09482
73-171	38	74.98	0.01470	0.07351
73-172	39	71.46	0.01944	0.09718
73-X	40	74.44	0.02395	0.11976
BFS-7010	41	72.14	0.01326	0.06629
BFS-7011	43	71.84	0.01371	0.06853
BFS-604	44	71.35	0.02247	0.11237
BFS-605	45	68.96	0.01326	0.06629
BFS-17A	46	60.36	0.01563	0.07817
BFS-17B	47	60.23	0.01645	0.08227

Average temperature at float altitude, 49.87°C.
Float altitude, approximately 36.6 km.
Launch date, May 8, 1974.
[a]Channel for which no temperature coefficient was provided.

Table 8. Summary of balloon flight 73-4 results compared with solar simulator measurements

Organization code	Module number	AMO, solar simulator (1 AU, 28°C)		Comparison, solar simulator and flight		Comments, postflight
		Preflight, mV	Postflight, mV	Preflight vs postflight, %	Flight vs preflight, %	
Goddard	73-012A[a]	79.07	79.02	0.06		None
Goddard	73-015[a]	67.40	67.60	-0.30		
Lewis	73-047[a]	55.20	55.12	0.14		
Lewis	73-051[a]	68.14	68.07	0.10		
Lewis	73-053[a]	46.20	45.93	0.58		
HAC	73-064	74.46	74.17	0.39	-0.43	
HAC	73-085	78.60	78.13	0.60	0.84	
HAC	73-086	77.82	77.49	0.42	0.70	
HAC	73-095	66.25	65.34	1.37	-0.46	
HAC	73-096	67.62	66.95	0.99	-0.73	
HAC	73-066	74.50	74.62	-0.16	0.88	
HAC	73-090	79.18	78.83	0.44	0.64	
HAC	73-091	76.10	75.81	0.38	-0.36	
JPL	73-183	68.32	67.81	0.75	-1.20	
HAC	73-093	75.62	75.43	0.25	-0.39	
HAC	73-0995	86.35	86.09	0.30	0.17	
JPL	73-181	68.76	69.20	-0.64	-0.85	
CRL	73-103[a]	75.20	74.70	0.66		
HEK	73-122	74.75	74.55	0.27	-0.31	
HEK	73-123	81.29	80.62	0.82	0.23	
ESTEC	73-136	58.30	57.97	0.57	0.68	
ESTEC	73-137	57.38	57.00	0.66	0.86	
ESTEC	73-141[a]	68.90	68.93	-0.04		
JPL	73-176	67.79	67.66	0.19	-1.11	
COMSAT	73-111	81.85	81.40	0.55	1.35	
TRW	73-180[a]	78.60	78.28	0.41		
JPL	BFS-505	66.10	66.28	-0.27	-1.11	
Marshall	73-034[a]	67.63	66.96	0.99		
JPL	73-171	75.06	75.10	-0.05	-0.10	
JPL	73-172	71.34	71.65	-0.43	0.17	
JPL	73-X	74.66	74.61	0.07	-0.29	
JPL	BFS-7010	71.70	71.70	0.00	0.61	
JPL	BFS-7011	71.72	71.73	-0.01	0.17	
JPL	BFS-604	72.02	71.80	0.31	-0.94	
JPL	BFS-605	69.68	69.70	-0.03	-1.04	
JPL	BFS-17A	60.17	60.55	-0.63	0.32	
JPL	BFS-17B	59.70	60.40	-1.17	0.89	

Average temperature at float altitude, 49.87°C.
Float altitude, approximately 36.6 km.
Launch date, May 8, 1974.
[a]Channel for which no temperature coefficient was provided.

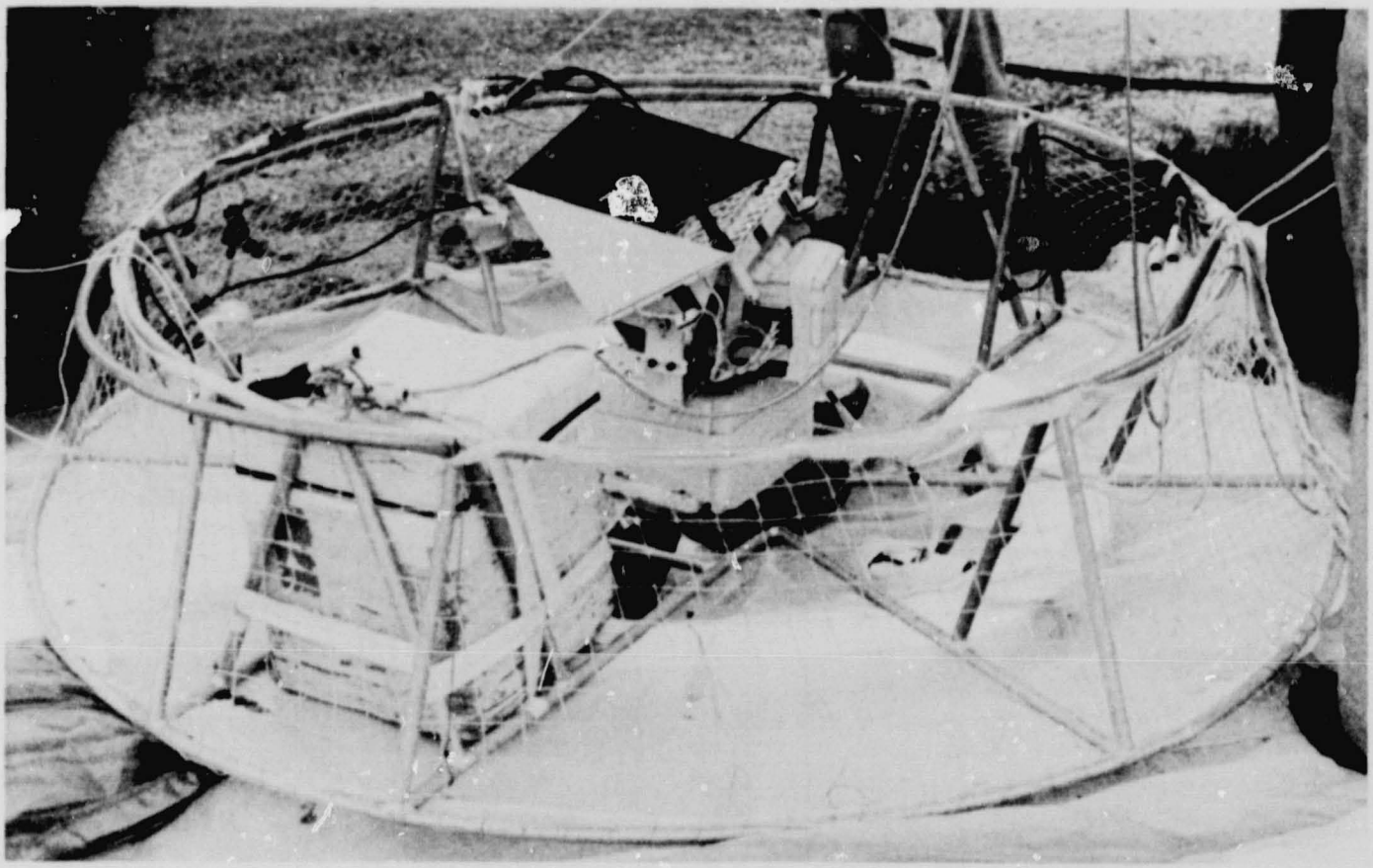

Fig. 9. Aluminum-hoop assembly with sun tracker in center

circular solar cell at the end of a 25.4-cm tube, is incorporated into the tracking platform. The cell is loaded near the short-circuit current point, and the millivolt output across the load resistor is fed to one of the telemetry channels. Thus, a high reading indicates an on-sun condition, while a low or zero reading indicates an off-sun condition.

A reflection shield is attached to the sun tracker to prevent unwanted reflected light from reaching the solar cell payload.

b. Solar cell modules. The solar cells selected for high-altitude calibration are assembled into standardized design packages in accordance with JPL Procedure No. EP 504443B (Ref. 2). An appropriate resistance is permanently fixed across the solar cell to load the cell near the short-circuit current point. Each module is carefully inspected for mechanical defects and electrically tested under solar simulation both prior to and following recovery of a successful balloon flight.

In addition to the normal solar cell modules, certain JPL modules have calibrated precision thermistors embedded in the copper substrate directly beneath the solar cell. These special modules are placed at strategic points on the sun tracker face and are used to determine the temperature of all other solar cell modules on a particular balloon flight. These special modules are flown on each flight to provide solar cell correlation data.

Solar cell modules are mounted onto the sun tracker platform with an interface of Dow Corning No. 340 silicone heat sink compound and held in place with four 2-56 screws. The heat sink compound is used to minimize thermal gradients between the two surfaces and to ensure the best possible uniform temperature on all solar cells comprising the payload.

c. Instrumentation circuit. The most practical method of measuring the short-circuit current of a solar cell is to load the cell near its short-circuit current point with a precision resistor and measure the voltage drop across the

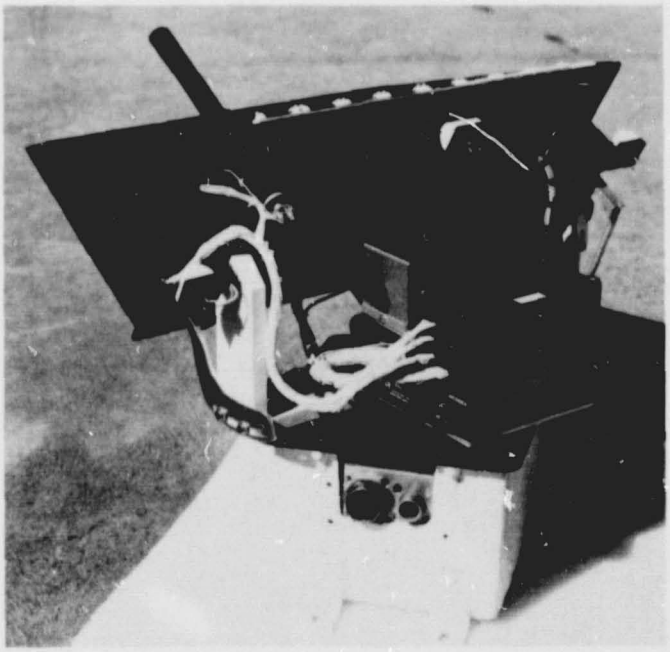

Fig. 10. Sun tracker

resistor (Fig. 11). Knowing the resistor value and the voltage reading, the short-circuit current may then be calculated.

In practice, the resistance value is chosen to place the cell output voltage reading in the upper portion of the 100-mV full-scale telemetry input range. Typically, the resistance values for the several sizes of solar cells manufactured are as shown in Table 9. The precision resistors used for standard solar cells have a temperature coefficient equal to or better than ±30 ppm/°C and a resistance stability equal to or better than ±0.002% over a three-year period.

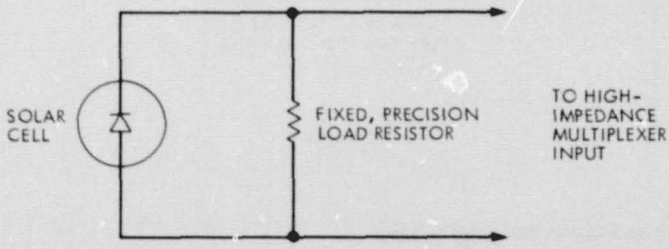

Fig. 11. Circuit diagram for measuring short-circuit current of solar cell

B. The Telemetry System

A major change was made in the data handling method from the method used in previous flight programs. A block diagram of past and present telemetry systems is shown in Fig. 12.

1. Airborne components. These components are described below.

a. Consolidated instrument package. The all-solid-state telemetry system is referred to as the Consolidated Instrument Package (CIP). This electronics package consists of a single command system, for both balloon control and scientific commands, and a telemetry system which has the capacity to handle all data transmissions on the flight over a common RF carrier. More specifically, the CIP contains the following equipment:

(1) Multiplexers (3) 100-mV full scale.

(2) Programmed Read Only Memory (PROM).

(3) Pulse-code-modulated (PCM) data encoder.

(4) PCM command receiver–decoder.

(5) Omega receiver.

(6) Rosemount pressure transducers.

(7) Subcarrier oscillators (as required).

(8) L-band FM transmitter.

(9) High-frequency tracking beacon transmitter (2).

A brief description of this capability as used by JPL is noted next. The PCM data encoder is of modular construction and has a main control unit which is used to determine bit rate, bits per word, parity, analog to digital conversion, and format. The format is controlled with a PROM which may easily provide a wide range of formats. Three 16-channel multiplexers have been included as part of the telemetry system to accommodate the low-level signals generated by the solar cells during flight. Each solar cell channel is read twice per second.

Table 9. Typical solar cell resistance values

Cell size, cm	Resistance value, ohms
1 X 2	1.000 ±0.1%
2 X 2	0.500 ±0.1%
2 X 4	0.250 ±0.1%
2 X 6	0.167 ±0.1%

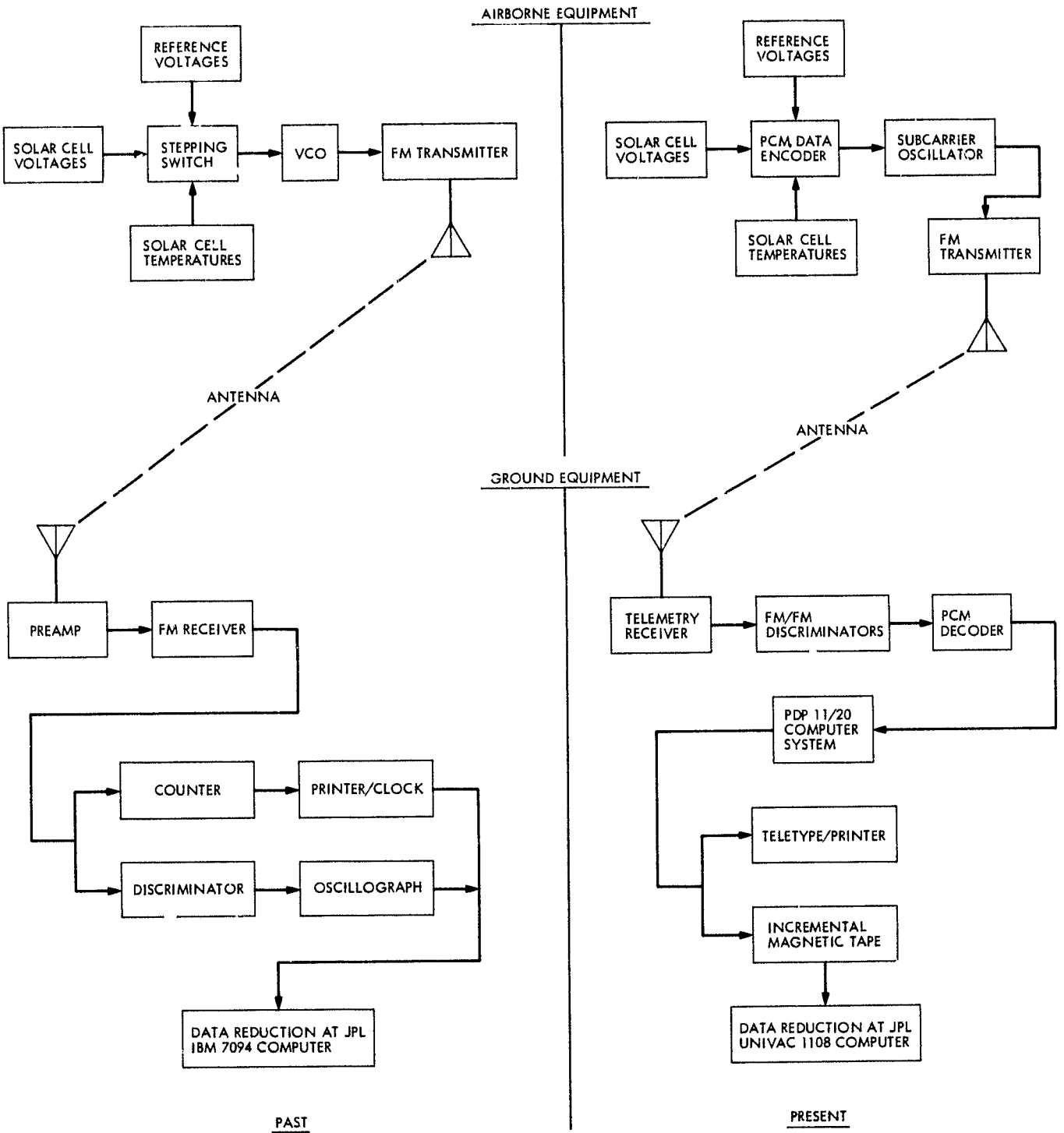

Fig. 12. Block diagram of past and present balloon telemetry system

The PCM command system is designed to be safe from false commands and is highly reliable in operation. The data is encoded on a frequency-shift-keyed audio carrier. This signal is then decoded into data and timing control. Each command consists of a double transmission of the data word. Both words must be decoded and pass a bit-by-bit comparison before a command is executed.

Altitude pressure is measured with a capacitance-type electronic transducer in the range of 102,000 to 40 N/m^2 (1020 to 0.4 millibars) that is accurate to 0.05%. This signal is a dc level which is encoded as PCM data and decoded at the receiving station into millibars.

The omega navigation system is used for flight tracking. An on-board receiver is used to receive the omega signal for retransmission to the processor in the ground station. This system can provide position data to less than 3.2 km.

A UHF L-band transmitter is used for data transmission to the ground station. In addition, a high-frequency beacon transmitter is used for aircraft tracking and altitude information after flight termination.

b. Battery power supply. Power for operating the electrical and electronic equipment on the balloon is supplied by a rechargeable battery source, although certain components such as radio beacons and other special equipment contain their own independent battery. The main battery pack is contained in the lower payload and supplies 28 Vdc regulated power and 36 Vdc unregulated power. The battery supply capacity is adequate to furnish power for a normal flight in addition to a reserve capacity.

2. Ground station, NSBF. The ground station at Palestine, Texas, is equipped with PCM data decommutation and real-time display equipment, omega processor, time code generator, time receivers (Loran and WWV), analog tape recorder, PDP-11/20 computer with incremental tape recorders, and PCM command encoders. A down-range station is maintained with the same equipment except for the computer. The composite telemetry signal is fed into the computer at the ground station to generate an incremental magnetic tape for processing at JPL using a Univac 1108 computer. The composite telemetry signal is also recorded directly onto magnetic tape as a backup and may be replayed through the PDP-11/20 computer to generate an incremental magnetic tape. The main purpose of the NSBF PDP-11/20 computer is to log data onto incremental tape.

A complete meteorological service organization, operated by NSBF personnel, is located at the National Scientific Balloon Facility for the sole purpose of providing weather information for balloon flights. A weather briefing is provided prior to each balloon flight, including forecasts for launch, ascent track to float altitude, float trajectory, descent track to impact, and recovery area weather.

C. The Balloon

The balloon employed for the JPL solar cell calibration high-altitude flights has a volume of 65,129 m^3 and is made from 1.78×10^{-5} m (0.7 mil) thick stratofilm, a polyethylene film designed for balloon use. The balloon is manufactured by Winzen Research, Inc., of Sulphur Springs, Texas. The balloon is designed to lift the weight of the sun tracker payload and other equipment to a float altitude of 36.6 km (120,000 ft). A multiconductor cable to electrically connect the top and bottom payloads is built into the balloon during the manufacturing process. A smaller tow balloon is used to stabilize the top-mounted payload during the launch phase.

Float altitude is maintained at 36.6 ± 0.6 km through the use of a radio-controlled ballast system attached to the lower payload.

VII. Balloon Flight and Payload Recovery

A. Balloon Launch

In typical balloon launch, the aluminum-hoop assembly with the sun tracker is attached to the top end fitting of the main balloon. The main balloon, protected by a plastic sheath, is laid out its full length on a ground cloth. The tow balloon is inflated and attached to the aluminum-hoop assembly with nylon lines. This tow balloon is used to stabilize the top-mounted payload during the launch phase.

The top end of a 8.5-m-diameter parachute is fastened to the balloon bottom end fitting. The lower payload, containing the consolidated instrument package, the battery power supply, and ballast for balloon control, is secured to the bottom of the parachute and all appropriate electrical connections made. The lower payload is attached with a quick-release mechanism to a launch vehicle.

When all checks and tests are completed, indicating proper operation of the balloon flight system, the main balloon is inflated. Helium is used as the lifting gas. Inflation is facilitated by a hydraulically operated high lift used to support the aluminum-hoop assembly. The helium is restricted to the upper portion of the balloon during

inflation by a mechanical launch arm. When sufficient helium is valved into the balloon, the high lift support is removed, and the aluminum-hoop assembly "floats" on the main balloon, supported partially by the tow balloon. Figure 13 shows the balloon flight system in the last stages of balloon inflation.

The balloon launch is achieved by first releasing the upper portion (bubble) of the balloon, the tow balloon acting as a stabilizer for the top-mounted payload. As the balloon rises, the launch vehicle maneuvers the lower payload directly beneath the balloon. The lower payload is released, and the entire balloon system is allowed to ascend as shown in Fig. 14. After the balloon has reached approximately 610 m, the tow balloon is released from the top-mounted payload. The ascent rate is normally 4.6 m/s; to reach float altitude of 36,576 m, slightly over two hours time is required.

B. Data Recording

The sun tracker is turned on by radio command once the balloon has reached float altitude. Experience has shown that while the balloon is ascending it rotates much faster than it does at float, and the sun tracker cannot always remain locked on the sun. Furthermore, the sun angle may be too low and out of the preset search angle during the early morning hours. Therefore, to save battery power and unnecessary wear on the tracker drive motors,

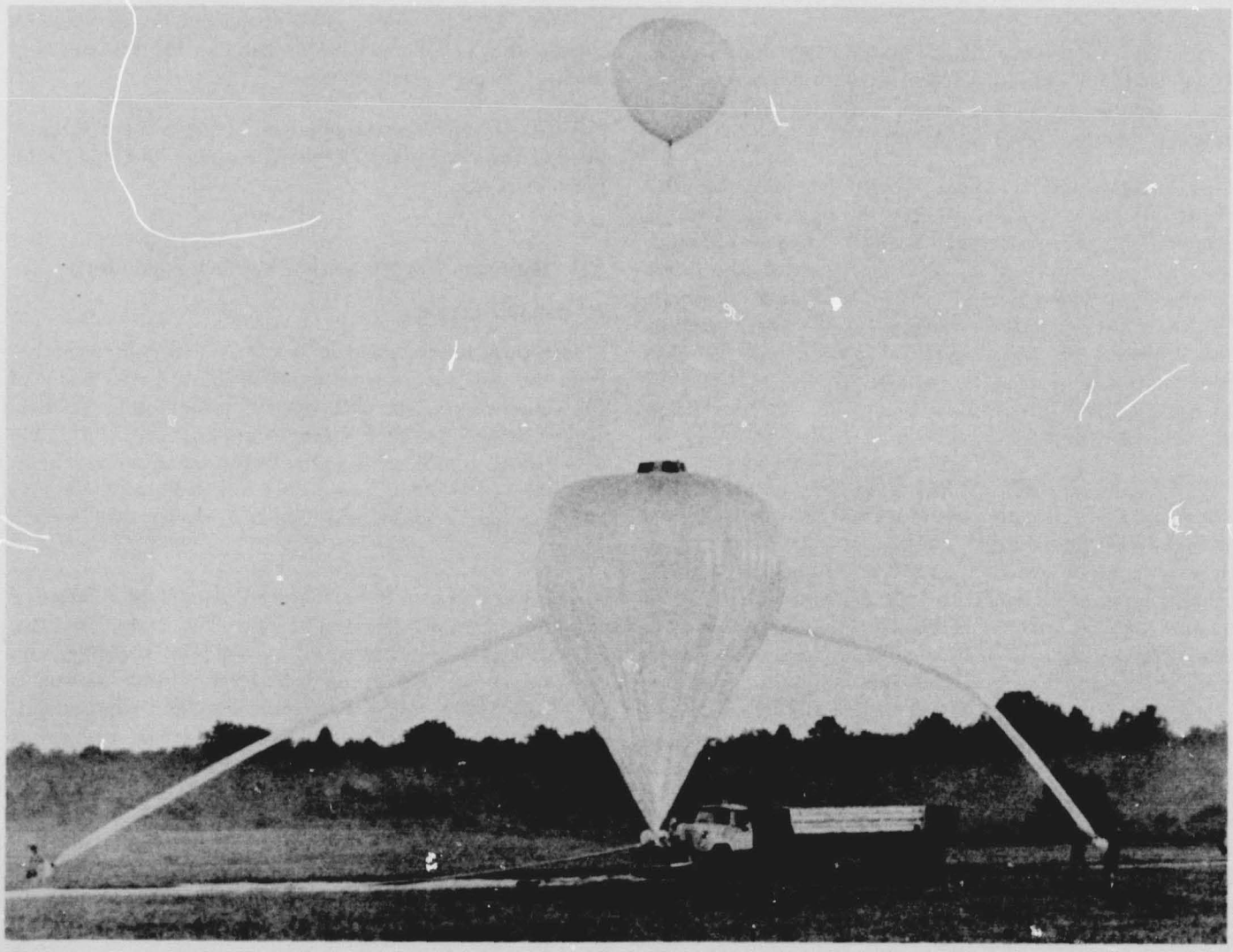

Fig. 13. Balloon inflation

Fig. 14. Balloon launch

the sun tracker is not turned on until the balloon reaches float altitude, about two hours prior to solar noon. Data is recorded continuously from two hours before solar noon until one hour past solar noon.

During the period in which the sun tracker is locked on the sun, solar cell voltages, interspersed with reference calibration voltages and thermistor voltages, are fed into the telemetry system. These voltages are converted to pulse code modulation (PCM) and are transmitted to a ground station where they are recorded on incremental magnetic tape for later processing at JPL and on the teletype for real-time assessment of the solar cells during data acquisition period.

C. Flight Termination

On balloon flights which are terminated several hundred miles from the launch site, the pilot of the tracking aircraft is responsible for conducting the flight termination sequence. When the pilot has a visual sighting on the balloon, a command is sent from the airplane to cut the steel hold-down cable and the electrical cable to the top payload. This action leaves the top payload resting on the balloon apex. Then a command is sent to cut the bottom payload loose from the balloon. As the payload falls away on its parachute, a rip line opens a large section of the balloon to ensure that the balloon itself will descend.

With the bottom payload released, the balloon is now top-heavy and rolls over, and the top payload slides off the top. As the aluminum-hoop assembly falls away, the parachute to this package is pulled out by a rip line attached to the balloon. The parachute is rigged to deploy and hold the aluminum-hoop assembly in an upright position to touchdown. During parachute descent, the pilot acts as the main spotter and directs the ground crew for recovery of the top and bottom payloads. The descent rate to touchdown is about 6.4 m/s. Since weather conditions play a vital role during the entire operation, both the top and bottom payloads are fitted with radio beacons to aid in their recovery. Once the payloads are on the ground, the recovery crew loads the packages onto the recovery vehicle and returns them to the launch site.

VIII. Data Reduction Procedure and Analysis

A. Task Description

Solar cell data, calibration data, and temperatures obtained in high-altitude balloon flights are transmitted to the ground in pulse code modulation (PCM counts) and recorded on magnetic tape. This program reads the data tape, converts solar cell readings to millivolts and

temperatures to degrees centigrade, and performs optional analysis of selected data. The computer print output consists of a tabulation of PCM counts for each scan processed, a tabulation of converted solar cell temperature data for individual channels, and averages, 95% confidence limits, and standard deviations for each solar cell channel.

B. Data Tape Input Procedure

Each magnetic tape record supplies data for 16 scans, or telemetry frames, followed by one ground frame. A telemetry frame is represented by 64 two-byte words on tape, consisting of 62 possible data channels followed by a 4-byte gap. Words 1, 7, 14, 21, 28, 35, and 42 are calibration channels; word 48 is the On-Sun indicator reading. The remaining 38 words between 1 and 48 are solar cell readings. Words 49 through 62 are not processed by the current version of the program. The first 8 words in the ground frame at the end of each record are the ASCII representation of time, GMT (in year, month, day, hour, minute, second, millisecond × 10, millisecond × 0.1).

Data is input from the tape, one record at a time, to provide data for a maximum of 100 scans to be processed for one flight in any one run. The tape is searched until the time closest to solar noon (or any specified time within the limits of the flight period) is found. The tape is then back-spaced to provide for input of approximately an equal number of scans before and after the time specified by the user. As the data is read in, a tabulation of readings in PCM counts for 48 channels of each scan is printed. A screening procedure rejects scans containing questionable data, and an explanatory message is printed out following each scan eliminated from further processing. For example, only those scans are used which were recorded during the time the sun tracker was locked on the sun as indicated by a predetermined output level of channel 48, the On-Sun indicator. When a total of 100 acceptable scans has been input, tape reading ceases and data is ready for further processing.

First, an additional check of data for each channel is made to detect changes in readings for adjacent scans exceeding an input increment. Excessive fluctuation is indicated by a flag preceding each questionable point in the output tabulation of converted individual readings by channel.

C. Data Conversion Procedure

The seven calibration readings are PCM counts corresponding to known voltages; linear interpolation is used to convert solar cell data from PCM counts to millivolts. The formula used is:

$$V = V_i + (PCM - PCM_i)\,[V_{i+1} - V_i/(PCM_{i+1} - PCM_i)]$$

$$\text{for } PCM_{i+1} \geq PCM \geq PCM_i$$

where (V_i, PCM_i) is a calibration voltage point with corresponding PCM count, and (V, PCM) is the interpolated point.

A preflight calibration procedure provides a temperature–PCM table to be used in converting the three temperature readings to degrees centigrade, using a similar linear interpolation method.

D. Output Calculations

A tabulation of the 100 accepted scans, for each of the 37 solar cell channels and 3 temperature channels, displays individual solar cell readings in millivolts and temperatures in degrees centigrade, with readings exceeding the input deltas of acceptable fluctuation being flagged with a preceding asterisk.

User input option provides for calculation of average, 95% confidence limits, and standard deviation for each solar cell channel. Four averages are computed for each channel: (1) an initial average based on 100 data points, (2) a corrected average using only points which fall within the limits of the initial average ± a specified per cent deviation, (3) the corrected average multiplied by the square of the ratio of the average radius vector to the current radius vector, and (4) a final temperature-corrected average. The second averaging procedure is designed to exclude from subsequent analysis any noticeably invalid points not eliminated by previous screening methods. Confidence limits and standard deviation are based on the final corrected average.

E. Contents of the Data Package

Following the final balloon flights and after the raw data has been reduced by computer, the standard solar cell calibration data is returned to the organizations that participated in the standardization program. The data package sent to the various participating organizations consists of a copy of the computer printout sheet depicting the serial number assigned to a given solar cell module and the average flight calibration value based on 100 data points corrected to 1 AU and a temperature of 28°C, provided that the participating organization has submitted a temperature coefficient value for its cell. Further, to aid in determining statistical validity of the results of tests, the 95% confidence limits are determined as well as the standard deviation.

IX. Systems Error Analysis

A. Error Sources

A brief study of the modified balloon flight measurement system elements (PCM telemetry data system) revealed four sources of error related to cell measurement, conversion of analog to digital data, and telemetry processing:

(1) Misorientation of the tracker with respect to solar normal incidence. The angle of misorientation θ of the solar tracker can result in short-circuit current error related by the cosine law correction. The percentage of the fractional error in short-circuit current measurement is given by

$$\frac{\Delta I_{sc}}{I_{sc}}\% = (1 - \cos\theta)\,100\%$$

(2) Load resistor accuracy. The resistors used to load the solar cells are precision-type with an accuracy of $\pm 0.1\%$. Therefore, the percentage of the fractional error in short-circuit current due to this source is given by

$$\frac{\Delta I_{sc}}{I_{sc}}\% = \pm 0.1\%$$

(3) Accuracy of the multiplexer-amplifier. Since multiplexer-amplifier accuracy is $\pm 0.5\%$, the percentage of the fractional error in short circuit current due to this source is given by

$$\frac{\Delta I_{sc}}{I_{sc}}\% = \pm 0.5\%$$

(4) Accuracy of the telemetry readout. The telemetry readout has 1023 counts for a full-scale output of 100 mV or

$$\frac{100\text{ mV}}{1023\text{ counts}} = 0.097775\text{ mV/count}$$

Therefore, a plus or minus 1 count would result in the following percentage of error at the corresponding data level:

$$100\text{ mV} = \pm 0.098\%$$
$$90\text{ mV} = \pm 0.109\%$$
$$80\text{ mV} = \pm 0.123\%$$
$$70\text{ mV} = \pm 0.140\%$$

The operating temperature variations between laboratory and field operation (25–55°C) are estimated to have negligible effect on the percentage of errors listed above.

B. System Mathematical Model

In order to determine the error from all the elements excluding the misorientation error, one must establish the system mathematical model and solve the equation that represents cell measurement, data conversion, and data processing. The system mathematical model is shown as follows:

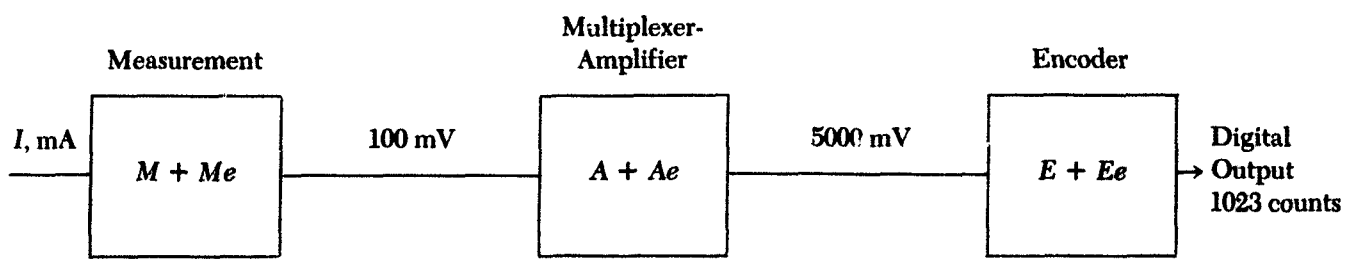

The conversion factor and the error of each element are shown inside each block:

$M + Me$ = measurement conversion factor

$$M = \frac{100\text{ mV}}{100\text{ mA}} = 1,\ Me = \pm 0.1\%$$

$A + Ae$ = multiplexer-amplifier amplification factor

$$A = \frac{5000\text{ mV}}{100\text{ mV}} = 50,\ Ae = \pm 0.5\%$$

$E + Ee$ = encoder conversion factor

$$E = \frac{1023}{5000\text{ mV}} = \frac{1}{4.9},\ Ee = \pm\ 0.098\%, 0.10\%$$

The system equation is

$$I\,(M + Me)\,(A + Ae)\,(E + Ee) = \text{digital count}$$

Solving Eq. (1) yields

$$(IM + IMe)\,(A + Ae)\,(E + Ee) = D$$

$$(IMA + IMAe + IMeA + IMe\,Ae)\,(E + Ee) = D$$

$$IMAE + IMAeE + IMeAE + IMeAeE + IMAEe$$
$$+ IMAeEe + IMeAEe + IMeAeEe = D$$

The above equation has two parts: (a) the unit representing the true digital count, and (b) units representing the error in digital count from the errors of the various sources:

$$D = IMAE + \text{errors}$$

$$\text{Errors} = \varepsilon = I(MAeE + MeAE + MeAeE + MAEe$$
$$+ MAeEe + MeAEe + MeAeEe)$$

Substituting the assigned numbers yields

$$M = 1, A = 50, E = \frac{1}{4.9}$$

$$Me = \pm 0.001 \qquad Ae = \pm 0.005,$$

$$Ee = \pm 0.00098, = \pm 0.001$$

$$\varepsilon = I\left[(1)(0.005)\frac{1}{4.9} + \frac{(0.001)\,50}{4.9} + \frac{(0.001)\,(0.005)1}{4.9}\right.$$
$$+ (1)50(0.001) + (1)\,(0.005)\,(0.001)$$
$$\left. + (0.001)\,(50)\,(0.001) + (0.001)\,(0.005)\,(0.001)\right]$$

Eliminating the insignificant factors (shown by x) the equation can be reduced to

$$\varepsilon = I\left[(0.001) + (0.010) + x + (0.05) + x + x + x)\right]$$

$$\varepsilon = I\left[(0.001) + (0.010) + (0.05)\right]$$

The above units have a $\pm$ value. Based on the above results, the digital count can be represented by

$$D = I\frac{(1)\,(50)}{4.9} + I\left[(\pm 0.001) + (\pm 0.010) + (\pm 0.05)\right]$$

$$= 10.23\,I \pm I \times \text{error}$$

where I = mA. For the case of 100 mA,

$$D = 10.23 \times 100 \pm 100 \times \text{error} = 1023 \pm 100 \times \text{error}$$

Data reduction of the computer printout includes a tabulation of the PCM count for each channel processed, the averages, the 95% confidence limits, and standard deviation. Four averages are computed for each channel: (1) an initial average based on 150 data points, (2) a corrected average using only points which fall within limits of the initial average $\pm$ a specified percent deviation, (3) a corrected average multiplied by the square of the ratio of the average radius vector, and (4) a final temperature-corrected average. Confidence limits and standard deviation are based on the final corrected average.

The initial averaging computation results in an rms value of the errors of

$$\varepsilon = \sqrt{(0.001)^2 + (0.010)^2 + (0.05)^2}$$

$$\varepsilon = 5.1 \times 10^{-2} = \pm 0.051$$

For the case of 100 mA,

$$D = 1023 + 100(0.051)$$

$$D = 1023 + 5.1$$

The percentage of error is given by

$$\frac{5.1}{1023} = 0.0048 = 0.50\%$$

Therefore, for the 100-mA measurement, the fractional error in short-circuit current is

$$\Delta I_{sc} = (0.0050)\,(100) = \pm 0.50 \text{ mA}$$

The second averaging computation will result in a corrected average value by eliminating a number of extreme data points. The corrected average will include only points which fall within the limits of the initial average ±3% deviation. Let us examine the mathematical relationship of the initial average and the corrected average.

1. Initial average. The data points are $D_1, D_2, D_3, \ldots, D_{150}$. The initial average is derived from the equation

$$\overline{D} = \frac{1}{150} \sum_{i=1}^{150} D_i$$

The measurement value is

$$M = \overline{D} \pm \sqrt{\epsilon_1^2 + \epsilon_2^2 + \epsilon_3^2}$$

where ϵ_1, ϵ_2, ϵ_3 are the error values found in the mathematical model.

2. Corrected average. The corrected average deletes all points that are

$$\frac{D_i}{\overline{D}} > 0.03$$

The corrected average therefore is derived from the equation

$$\hat{\overline{D}} = \frac{1}{K} \sum_{i=1}^{K} D_i$$

where K is the value of the data points remaining. For the first approximation, and since the errors calculated are small, the new measurement value is

$$Mz = \hat{\overline{D}} + (1 - \eta)\sqrt{\epsilon_1^2 + \epsilon_2^2 + \epsilon_3^2}$$

where

$$\eta = \frac{\overline{D} - \hat{\overline{D}}}{\overline{D}}\%,$$

where η = the percent difference of the averages, which means that if the corrected value is within a small percentage of the initial average, then the error is reduced by the factor $(1 - \eta)$. For example, if the corrected value is at 95% of the initial value, then the error is corrected by $(1 - 0.05) = 0.95$. Therefore, for the case of 100 mA the error in short-circuit current is (0.95) (0.50 mA) = 0.475 mA, which equals ±0.475%. In case of larger average difference, the first approximation will not hold.

C. Conclusion

The accuracy of the balloon flight telemetry measurement is within ±0.50% of the actual reading (short-circuit current) for 100-mA measurement by averaging the data points and is reduced to ±0.475% by the corrected average computation if the corrected average is within 95% of the initial average. The biggest portion of this error is attributed to the multiplexer amplifier gain factor and associated error.

X. Conclusions

Solar cell calibration using the high-altitude balloon flight technique has been performed by JPL since 1962. Table 10 provides a list of data gathered on one particular standard solar cell (BFS-17A) over a nine-year period (Ref. 3). This cell was used as a reference on nearly every balloon flight including those discussed herein and has repeated its average calibration value in each instance to better than 1%. From this data, two conclusions can be stated: (1) that the balloon flight system has maintained excellent stability over the years, and (2) that silicon solar cells are reliable as standards over a long term if properly maintained. Another important conclusion established from these series of balloon flights is that new high-efficiency cells which have increased spectral response characteristics beyond the region of 0.4 to 1.2 micrometers—or, more specifically, have increased enhancement

between 0.3 to 0.6 micrometers—have shown significant increase in earth-space efficiencies. However, these increases can also be readily detected to within 1.5% under present-day close filtered xenon solar simulators. The solar cell calibration program is a continuing program designed to fill the need for AMO calibrated solar cells. The use of high-altitude balloons has once again proved to be a feasible, reliable, and economical method of obtaining data on newly developed photovoltaic devices as well as typical production-type standards.

Table 10. Repeatability of standard solar cell BFS-17A for 23 flights over a 9-year period

Flight date	Output, mA	Flight date	Output, mA
9/5/63	60.07	8/4/67	59.83
8/3/64	60.43	8/10/67	60.02
8/8/64	60.17	7/19/68	60.31
7/28/65	59.90	7/29/68	60.20
8/9/65	59.90	8/26/69	60.37
8/13/65	59.93	9/8/69	60.17
7/29/66	60.67	7/28/70	60.42
8/4/66	60.25	8/5/70	60.32
8/12/66	60.15	2/16/74	59.73
8/26/66	60.02	4/5/74	60.37
7/14/67	60.06	4/23/74	60.37
7/25/67	60.02	5/8/74	60.36

Average $\overline{X}$ = 60.16

Maximum deviation from $\overline{X}$ = 0.8%

Each data point is an average of 20-30 data points from flight for period 9/5/63 to 8/5/70.

For flights beginning in 2/16/74, each data point is an average of 100 or more data points from each flight.

All data are normalized to 1 AU and to a cell temperature of 301.15 K (28°C).

References

1. Gast, P. R., "Solar Radiation," in *Handbook of Geophysics*, C. F. Campen, Jr., et al., eds. Chapter 16:14-32, MacMillan Co., New York, 1960.
2. Greenwood, R. F., "Solar Cell Modules, Balloon Flight Standard, Calibration of," Procedure No. EP 504443, Revision B, Jet Propulsion Laboratory, Pasadena, California, February 5, 1969 (JPL internal document).
3. Greenwood, R. F., and Mueller, R. L., *Results of the 1970 Balloon Flight Solar Cell Standardization Program*, Technical Report 32-1575, Jet Propulsion Laboratory, Pasadena, California, December 1, 1972.

NASA—JPL—Coml., L.A., Calif.